COMPARISON OF COMPUTATION METHODS

FOR CBM PRODUCTION PERFORMANCE

A Thesis

by

CARLOS A. MORA

Submitted to the Office of Graduate Studies of
Texas A&M University
in partial fulfillment of the requirements for the degree of

MASTER OF SCIENCE

August 2007

Major Subject: Petroleum Engineering

COMPARISON OF COMPUTATION METHODS

FOR CBM PRODUCTION PERFORMANCE

A Thesis

by

CARLOS A. MORA

Submitted to the Office of Graduate Studies of
Texas A&M University
in partial fulfillment of the requirements for the degree of

MASTER OF SCIENCE

Approved by:

Chair of Committee,   Robert A. Wattenbarger
Committee Members,   Bryan Maggard
                        Prabir Daripa
Head of Department,   Stephen A. Holditch

August 2007

Major Subject: Petroleum Engineering

ABSTRACT

Comparison of Computation Methods for CBM Production Performance. (August 2007)

Carlos A. Mora, B.S., Universidad de America

Chair of Advisory Committee: Dr. Robert A. Wattenbarger

Coalbed methane (CBM) reservoirs have become a very important natural resource around the world. Because of their complexity, calculating original gas in place and analyzing production performance require consideration of special features.

Coalbed methane production is somewhat complicated and has led to numerous methods of approximating production performance. Many CBM reservoirs go through a dewatering period before significant gas production occurs. With dewatering, desorption of gas in the matrix, and molecular diffusion within the matrix, the production process can be difficult to model.

Several authors have presented different approaches involving the complex features related to adsorption and diffusion to describe the production performance for coalbed methane wells. Various programs are now commercially available to model production performance for CBM wells, including reservoir simulation, semi-analytic, and empirical approaches. Programs differ in their input data, description of the physical problem, and calculation techniques.

This study will compare different tools available in the gas industry for CBM reservoir analysis, such as numerical reservoir simulators and semi-analytical software programs, to understand the differences in production performance when standard input data is used. Also, this study will analyze how sorption time (for modeling the diffusion process) influences the gas production performance for CBM wells.

DEDICATION

This work is dedicated to my mother, Cecilia Sanchez, and in memory of my father, Cesar Mora (rest in peace), for their love and support. They have provided me with good examples of determination, strength and faith in God.

This work is also dedicated to my brothers for their encouragement.

ACKNOWLEDGEMENTS

TABLE OF CONTENTS

LIST OF TABLES

LIST OF FIGURES

CHAPTER I

INTRODUCTION

1.1 Problem Description

The flow mechanics of coalbed methane (CBM) production have some similarities to the dual porosity system. This naturally fractured reservoir is characterized as a system of matrix blocks with each matrix block surrounded by fractures (cleats). The fluid drains from the matrix block into the cleat system which is interconnected and leads to the well. Warren and Root[1] introduced a mathematical model for this dual porosity matrix/fracture behavior. Their model has been widely used for many types of reservoirs, including tight gas and coalbed methane reservoirs. Fig. 1.1 compares the actual reservoir and its idealization model where the matrix and the cleat systems can be differentiated. Also, three sets of normal parallel fractures are shown (face cleats, butt cleats and bedding plane fractures).

Actual Reservoir   **Model Reservoir**
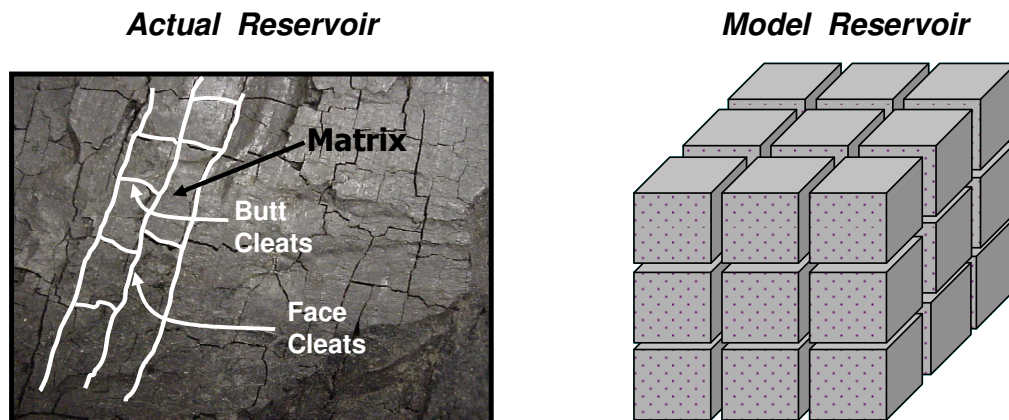
Figure. 1.1 Actual and Model CBM Reservoir.

_____

This thesis follows the style of the *Society of Petroleum Engineers Journal*.

CBM models are characterized as a coal/cleat system of equations. Most of the gas is stored in the coal blocks (adsorption). Gas desorbs in the coal block and then drains to the fracture system by molecular diffusion (Fick's Law rather than Darcy's Law). The diffusion process can be represented by means of the sorption time, τ. By definition, τ, is the time at which 63.2% of the ultimate drainage occurs when maintained at constant surrounding pressure and temperature.

The typical production profile for a CBM well is shown in Fig. 1.2. The production behavior exhibit only water production from the cleat system at the beginning (Flow through the cleat system is governed by Darcy's Law), then, due to the reduction in formation pressure, gas starts to desorbs from the matrix creating a concentration gradient; and gas and water flow through the cleat system. Water rate decreases and the Gas rate increases until the gas peak is reached (the gas production behavior in this stage is dominated by diffusion). Finally, when depletion in the reservoir is significant, the gas rate declines. Because reservoir pressure is reduced during production, porosity and permeability in the system are reduced (matrix shrinkage).
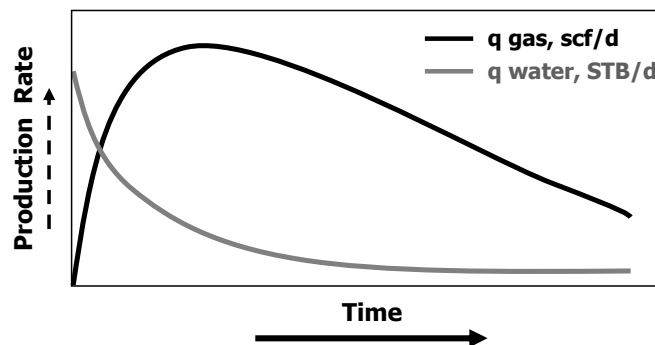
Figure. 1.2 Typical Production Profile for a CBM Well.

For Dry coal reservoirs (no water in the cleat system) there is no dewatering period (no gas peak). Free gas is produced at the beginning and when the pressure decreases gas starts to desorbs from the matrix and flow towards the cleat system (desorption/diffusion). The production profile for wells draining these dry coal reservoirs tends to be similar to those from wells producing from conventional gas reservoirs (gas rate declines from the beginning).

Several authors have presented different approaches involving the complex features related to adsorption and diffusion to describe the production performance for coalbed methane wells. Various programs are now commercially available to model production performance for CBM wells, including reservoir simulation, semi-analytic, and empirical approaches. Programs differ in their input data, description of the physical problem, and calculation techniques.

1.2 Literature Review

Several authors have presented different approaches to describe the production performance for coalbed methane wells.

Zuber[2] pointed out that history matching analysis can be used to determine CBM reservoir flow parameters and predict performance by using a simulator modified to include storage and flow mechanisms. The history matching analysis using a two-phase, dual porosity simulator includes laboratory, geologic and production data for determining reservoir properties.

Later work by Seidle[3] suggested conventional reservoir simulation with some modifications in the input data for modeling coalbed methane reservoirs. His approach

assumes instantaneous desorption from matrix to cleats for modeling adsorption of the gas in the surface of the coal as gas dissolved in an immobile oil. The solution gas oil ratio is calculated using the Langmuir isotherm, Fig. 1.3. Some modifications in the input data (porosity and gas-water relative permeability curves) have to be applied due to the presence of the "immobile" oil. However, no code modifications in the simulator are required. This method was verified by using conventional black oil reservoir simulators and compared with CBM Reservoir simulators developed during that time.
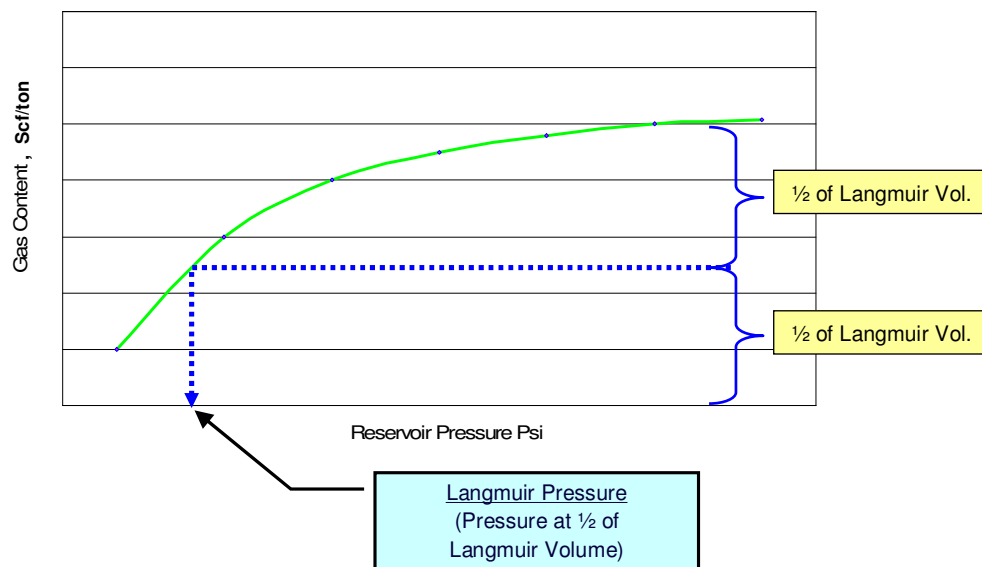
Figure. 1.3 Langmuir Isotherm Curve.

King[4] presents a modified material balance technique for estimating the original gas in place and future well performance for unconventional gas reservoirs. This method uses the traditional assumptions for the material balance (M.B.) approach but also considers effects of adsorbed gas and gas diffusion. The M.B. technique assumes equilibrium between free gas and absorbed gas in the coal and pseudo-steady state process during sorption. The

method is suggested to estimate Gas in place (*p/Z* method) and for production predictions based on M.B. methods for conventional gas reservoirs including effects of adsorbed gas. According to this technique, Gas in Place can be determined using Eq. 1.1.

$$OGIP = Ah\phi \frac{T_{sc} Z_{sc}}{P_{sc} T} \left[\frac{p_i}{Z_i^*} \right]$$ ……………………………………..………………… 1.1

This Equation in material balance form results in Eq. 1.2:

$$\frac{P}{Z^*} = \frac{P_i}{Z_i^* (OGIP)} G_p + \left[\frac{p_i}{Z_i^*} \right]$$ ……………………………………………..…… 1.2

Z^* represents the gas factor for unconventional gas reservoirs which is defined using Eq. 1.3:

$$Z^* = \frac{Z}{\left[1 - c_f (p_i - p)\right](1 - \overline{S_w}) + \frac{\rho_b}{\phi} \frac{V_L P}{P_L + P}}$$ ……….………………………………… 1.3

The Material balance interpretation from Eq. 1.2 is given by a straight line in *p/Z** as is shown in Fig. 1.4.
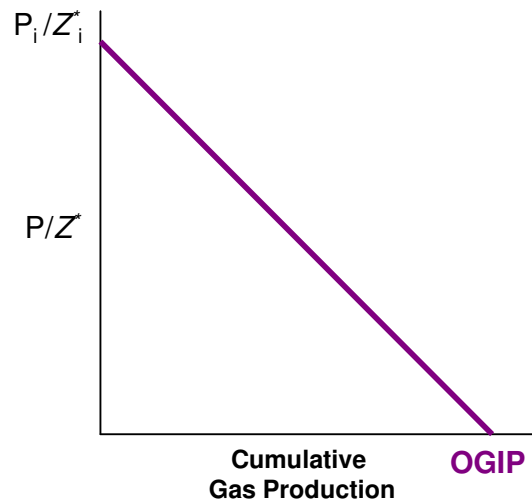
Figure. 1.4 P/Z * Plot

Seidle[5] and Jensen & Smith[6] presented modifications to King's method. Seidle's suggests a more robust material balance method, improving King's M.B. method including mathematical development, simulation studies and field examples. The modified method eliminates mathematical problems from the original method, to obtain a more accurate OGIP determination for coalbed methane reservoirs. Jensen and Smith's method assumes the gas stored in the cleat system is negligible (no water saturation effects).

Papers by David and Law[7], Hower[8], and Jalal and Shahab[9] showed how numerical compositional simulators with additional features can be used for coalbed methane modeling. David and Law[7] presented a comparison study using numerical simulation for modeling enhanced recovery in CBM reservoirs with CO_2 injection. The numerical compositional simulators handle two or more components. Also conventional oil or gas compositional simulators were used to model CBM recovery processes by using a single-porosity approach assuming that the gas diffusion from matrix to fractures is instantaneous.

Aminian *et al.*[10] introduced a new alternative to predict coalbed methane production performance using a set of gas and water type curves. This technique uses dimensionless rate and time for water and gas. From the above study it was concluded that type curves can be used for production history matching to determine initial matrix content and cleat porosity. This technique generates predictions of future production rates and can be also used to predict production performance of CBM prospects. Besides this, a correlation for peak gas rate is developed in this study for production predictions.

Nowadays, different reservoir simulators and semi-analytic software programs using the methods described above are available in the industry to predict production performance for CBM wells.

CHAPTER II

COMPUTATION METHODS FOR MODELING CBM

2.1 Description of Computation Methods

Commercial reservoir simulators like GEM (Computer Modeling Group, CMG) and Eclipse[11] (Schlumberger) have incorporated sorption and diffusion processes, coal shrinkage, compaction effects, and under-saturated coals to their dual porosity models. The models can handle two gas systems (typically CO_2 and methane) in both primary production and injection modes. Besides, simple and complex well completions such as multi-branch horizontal wells and hydraulic fracture treatments can be simulated.

The CBM model used for numerical simulators applies a modified Warren and Root[1] dual porosity model to describe the physical processes involved in coalbed methane projects. The adsorbed concentration on the surface of the coal is assumed to be a function of pressure only (Langmuir isotherm). The diffusive flow of gas from the coal matrix is given by Fick's Law.

Jalali and Shahab[9] from West Virginia University designed a new simulator for Independent producers using King,s[4] formulation. This model is single-well radial and it generates production forecast, and volumetric calculations.

Semi-analytical software programs are also available for modeling CBM wells. F.A.S.T. CBM is a semi-analytic model from Fekete Associates Inc. For modeling CBM wells, this program combines desorption (Langmuir Isotherm) and equations for conventional gas reservoirs[12]. This software has been developed to estimate reserves and generate production forecasts for CBM Wells. The software mainly includes Volumetric

Gas in Place calculations (adsorbed gas and free gas) and Langmuir isotherm for recovery factor and recoverable reserves estimation based on abandonment pressure. The software also includes decline analysis for alternative estimation of gas in place, optional matrix shrinkage for forecasting/history matching and material balance calculations using different techniques (King[4], Seidle[5], Jensen & Smith[6]). Besides this, production predictions can be evaluated using multi-well and multi-layer analysis.

PRODESY is a semi-analytic software program from Rapid Technology Corporation. For modeling CBM wells, this program combines reservoir analysis methods for conventional gas reservoirs and desorption. The software includes the option for modeling horizontal wells in coalbed methane reservoirs.

PROMAT (Schlumberger) is another available software program. This software use a single phase solution for modeling dry coal reservoirs (no water in the cleat system).

Generally speaking, to model CBM wells, semi-analytical software programs apply the same equations used for conventional reservoirs. However, the production from the matrix is a function of the Langmuir isotherm. The effects of adsorption combined with two-phase flow generate the characteristic production curves for this type of wells.

2.2 Differences in the Input Data

Simulators and programs differ in their input data, description of the physical problem, and calculation techniques.

GEM (Computer Modeling Group, CMG): For modeling the diffusion process, GEM uses Sorption Time, τ, as a direct input. Even though, the cleat spacing must be an

input for running the simulator (sigma is calculated by using the available options in the simulator, Warren & Root[1] or Kazemi[13]), this spacing does not affect the input value for sorption time.

ECLIPSE: The required Input data for modeling the diffusion process consist on the diffusion coefficient (D_c) and shape factor, σ. Sorption time is then calculated combining the shape factor and the diffusion coefficient. Sigma has to be calculated by hand (Formulas from Mora and Wattenbarger[14], Appendix A, are recommended for calculating σ value).

The semi-analytical software programs (F.A.S.T., CBM, PRODESY, and PROMAT) do not include diffusion process for their CBM models (Fick's Law is not used); so, sorption time is not an input for CBM reservoir analysis in these programs.

Desorption process is modeled for numerical simulators and semi-analytical software programs using the Langmuir isotherm equation which assumes that the concentration of methane adsorbed on the surface of coal matrix is a function of pressure only.

2.3 GIP Estimation for CBM Reservoirs

CBM models are characterized as a coal/cleat system of equations. Most of the gas is stored in the coal blocks. Gas storage is dominated by adsorption according to Eq. 2.1.

$$GIP_s = A * h * (1-\phi) * \rho_b * G_c \quad \text{...} \quad 2.1$$

Gas concentration, G_c, is a function of the Langmuir Isotherm curve by means of Eq. 2.2:

$$G_c = \frac{V_L \cdot p}{p_L + p} \quad \text{...} \quad 2.2$$

Langmuir volume (V_L) represents the maximum amount of methane adsorbed on the surface of the coal matrix when the pressure, p, reaches infinity. This value is asymptotically approached by the isotherm (Fig. 1.3) as the pressure increases.

Langmuir pressure (p_L) represents the pressure where the amount of adsorbed methane is one half of its maximum amount, V_L.

For most of the reservoirs, the coal cleats are initially water saturated. However, some reservoirs present free gas in the cleat system, and in some special cases, there is no water in the cleat system (dry coal).

Most of the times, the free gas in the cleat system volume is very small compared with the gas adsorbed on the surface of the matrix.

Gas in Place in the cleat system is estimated using the volumetric Eq. 2.3.

$$GIP_f = A * h * \phi * (1\text{-}S_w) / \beta_g \quad \text{……...……………………………………...…………}\quad 2.3$$

So, the total gas in place is the sum of the adsorbed gas in the matrix system and the free gas in the cleats as is shown in Eq. 2.4.

$$GIP = GIP_s + GIP_f \quad \text{………………...………………………………...…………}\quad 2.4$$

CHAPTER III

SORPTION TIME FOR MODELING DIFFUSION PROCESS

Gas desorbs in the coal block and then drains to the fracture system by molecular diffusion (Fick's Law rather than Darcy's Law). The drainage rate (Fick's Law) from the coal block can be expressed using Eq. 3.1:

$$q^* = \sigma \cdot D_c \cdot (\bar{c} - c_f) \qquad \dots\dots\dots\dots\dots\dots\dots\dots\dots\dots\dots\dots\dots\dots\dots\dots\dots\dots \quad 3.1$$

For Eq. 3.1, q^* represents drainage rate per volume of reservoir. For modeling CBM reservoirs sorption time, τ, is used. Sorption time is related to the transfer shape factor, σ, and the Diffusivity coefficient, D_c. Sorption time, τ, express the diffusion process by means of Eq. 3.2:

$$\tau = \frac{1}{\sigma \cdot D_c} \qquad \dots\dots\dots\dots\dots\dots\dots\dots\dots\dots\dots\dots\dots\dots\dots\dots\dots\dots\dots\dots \quad 3.2$$

Appendix B shows the derivations for CBM/Fick's Law relating Shape Factor, Tau, and the diffusivity coefficient.

By definition, τ, is the time at which 63.2% of the ultimate drainage occurs when maintained at constant surrounding pressure and temperature.

From laboratory tests[15] (canister test) the diffusivity term can be estimated, and by applying Eq. 3.2 the sorption time can be calculated.

Numerical reservoir simulators use diffusion (sorption time) in their models. However, this parameter is calculated from different existing formulations in literature.

Sorption time formulation was presented by Zuber[2] by means of Eq. 3.3:

$$\tau = \frac{L^2}{8 \cdot \pi \cdot D_c}$$ …………………..………………………………………………………… 3.3

Sorption time estimation is suggested by Ticora[15] (Laboratory reports) according to Eq. 3.4:

$$\tau = \frac{1}{\frac{15}{r^2} \cdot D_c}$$ ……………...……………………………………………………………… 3.4

Also, commercial reservoir simulators suggest modeling diffusion process according to Eq. 3.2, but applying either Warren and Root[1] or Kazemi[13] formulations for shape factor, which results in Eq. 3.5 and Eq. 3.6 for Warren and Root[1] and Kazemi[13] respectively.

$$\tau = \frac{1}{\frac{4n(n+2)}{L^2} \cdot D_c} = \frac{1}{\frac{60}{L^2} \cdot D_c}$$ …..……………………………………………… 3.5

$$\tau = \frac{1}{4\left(\frac{1}{L_x^2} + \frac{1}{L_y^2} + \frac{1}{L_z^2}\right) \cdot D_c} = \frac{1}{\left(\frac{12}{L^2}\right) \cdot D_c}$$ ..……………………………………… 3.6

From Mora and Wattenbarger[14], the term $(8\pi/L^2)$ from Eq. 3.3 is related to the shape factor for cylindrical geometry draining at constant rate.

Also, the term $(15/r^2)$ from Eq. 3.4 belongs to the shape factor for spherical geometry (constant rate case).

Eq. 3.5 and Eq. 3.6 are based on Eq. 3.2, but the shape factor, σ, correspond neither to the geometry nor to the boundary condition. These equations (3.5 and 3.6) were suggested for geometry of three sets of normal parallel fractures and equal fracture spacing but according to Mora and Wattenbarger[14] these formulations are incorrect.

By using the shape factor formulas suggested by Mora and Wattenbarger[14], in Eq. 3.7, for a desorption process at constant concentration, sorption time can be correctly expressed as follows:

$$\tau = \frac{1}{\pi^2 \left(\dfrac{1}{L_x^{\,2}} + \dfrac{1}{L_y^{\,2}} + \dfrac{1}{L_z^{\,2}} \right) \cdot D_c} \qquad \text{..} \qquad 3.7$$

Eq. 3.7 belongs to geometry of three sets of normal parallel fractures. For equal fracture spacing, τ, Eq. 3.8 is obtained.

$$\tau = \frac{1}{\left(\dfrac{3\pi^2}{L^2} \right) \cdot D_c} \qquad \text{..} \qquad 3.8$$

CHAPTER IV

COMPARATIVE CASES

For this comparison study two different reservoir simulators (GEM and ECLIPSE) and three different software programs (F.A.S.T CBM, PRODESY, and PROMAT) have been selected. These tools were selected due to its availability for academic purposes. Fig. 4.1 shows a sketch of the methodology used for the comparison study.
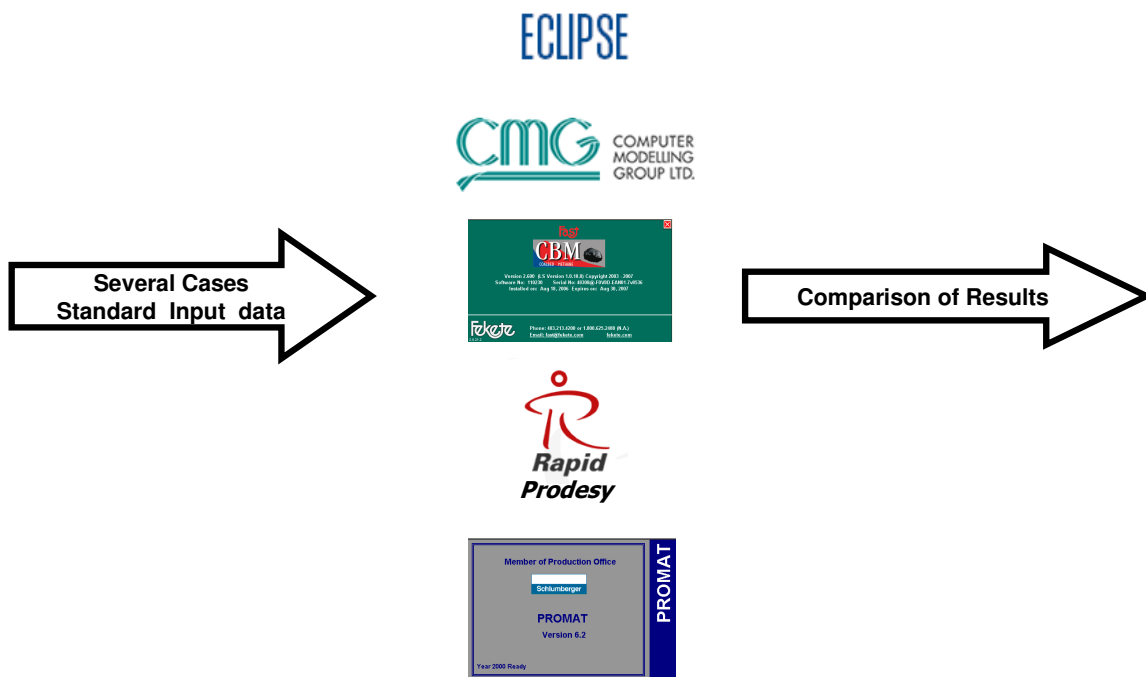

Figure. 4.1 Methodology for the Comparison Study.

For comparing the different computational tools, several test cases have been analyzed. The cases belong to single vertical wells, vertical hydraulic fractured wells, and horizontal wells. These cases have been chosen because these are the techniques used for drilling & completion for CBM wells.

A summary of the different test cases is shown in Table 4.1.

TABLE 4.1 SUMMARY OF TEST CASES USED FOR COMPARISON			
Case	Description	Source Data	Computation Methods
Case 1	Single Vertical Well	Synthetic data	Eclipse, GEM, Rapid, Fekete
Case 1b	Case 1 (Dry Coal)	Synthetic data	Eclipse, GEM, Rapid, Fekete, Promat
Case 2	Vertical Hydraulic Fractured Well	Synthetic data	Eclipse, GEM, Rapid, Fekete
Case 2b	Case 2 (Dry Coal)	Synthetic data	Eclipse, GEM, Rapid, Fekete
Case 3	Horizontal well	Synthetic data	Eclipse, GEM, Rapid
Case 3b	Case 3 (Dry Coal)	Synthetic data	Eclipse, GEM, Rapid
Case 4	Vertical Hydraulic Fractured Well	Real Field Example	Eclipse, GEM
Case 5	Horizontal well	Real Field Example	Eclipse, GEM
Case 6	Multi-well	Synthetic data	Eclipse

Case 1 describes a single vertical well, Case 2 corresponds to a vertical fractured well, and Case 3 corresponds to a horizontal well. These cases consider the cleat system initially fully water saturated. Cases 1b, 2b, and 3b are same Cases 1, 2, 3 respectively but for modeling dry coal (no water in the cleat system). Cases 1, 1b, 2, 2b, 3, and 3b were modeled using realistic synthetic data. To establish the impact in gas production performance using the existing formulations for sorption time in the industry, cases 4 and 5 are analyzed (real examples from a CBM reservoir in Oklahoma). Case 6 is a multi-well case using synthetic data.

Case 1

Fig. 4.2 shows the model geometry for this test case (single radial model). Table 4.2

shows the input parameters used for this case (the check marks refers to the required input

data). Original Fluids in place and production recovery are presented for each case as well.

It can be observed that the computation methods differ in their input data. Numerical

simulators apply Fick's Law (input τ or D_c) but the software programs do not.

Vertical Well

Fracture PERMR

5.0000   5.0000

Figure. 4.2 Model Geometry Case 1 (Single Vertical Well).

TABLE 4.2 RESERVOIR PARAMETERS FOR CASE 1					
Parameter	Value	PRODESY	F.A.S.T. CBM	GEM	ECLIPSE
Area, Ac	80	✓	✓	✓	✓
Thickness, ft	12.5	✓	✓	✓	✓
Initial Average Pressure, psia	700	✓	✓	✓	✓
Fracture porosity, %	1	✓	✓	✓	✓
Water Saturation (Fractures), %	100	✓	✓	✓	✓
Coal Density, gm/cc	1.5	✓	✓	✓	✓
Fracture Permeability, md	5	✓	✓	✓	✓
Langmuir Pressure, psia	100	✓	✓	✓	✓
Langmuir Volume, scf/ton	591	✓	✓	✓	✓
Well Bottom-hole pressure, psia	50	✓	✓	✓	✓
Temperature, °F	70	✓	✓	✓	✓
Sorption Time. days				200	
Diffusion Coefficient, ft^2/d					7.246 e-7
Sigma, ft^{-2}					6,900
Gas in Place, Bscf		1.055	1.055	1.055	1.055
Water in Place, STB		N/A	N/A	77,847	77,966
Cum. Gas Production @20 years, MMscf		296	296	320	309
Recovery Factor, %		28	28	30.3	29.3

Case 2

For case 2 (vertical fractured well), infinite conductivity in the hydraulic fracture was modeled because the software programs assume infinite conductivity in their models. Fig. 4.3 shows the model geometry for this test case. Table 4.3 shows the input parameters used for this case (the check marks refers to the required input data). It can be observed that the computation methods differ in their input data. Numerical simulators apply Fick's Law (input τ or D_c) but the software programs do not.
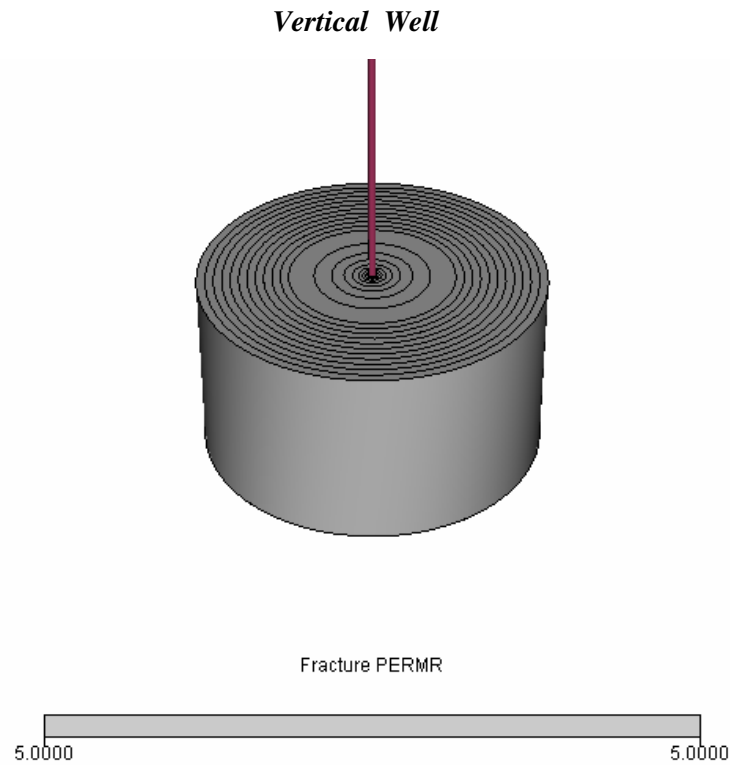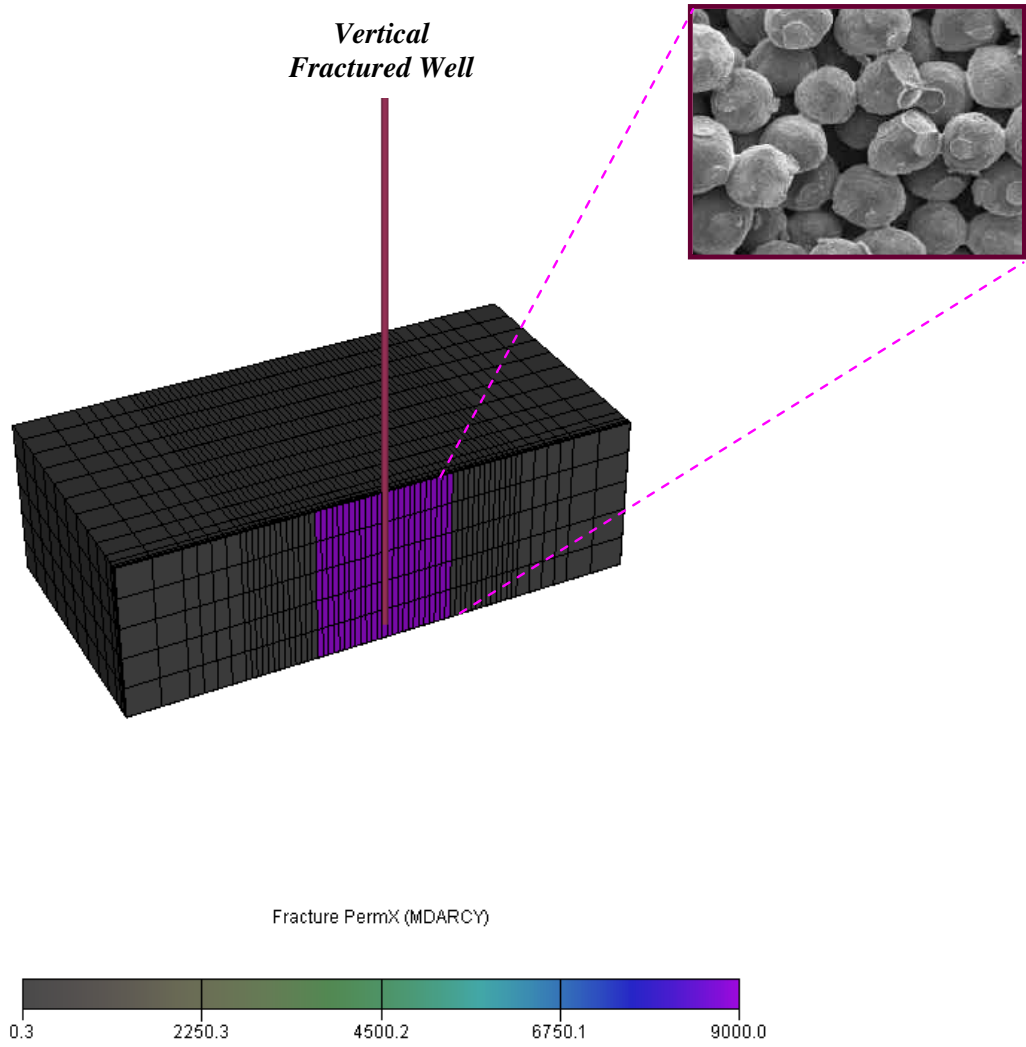
Figure. 4.3 Model Geometry Case 2 (Vertical Hydraulic Fractured Well).

TABLE 4.3 RESERVOIR PARAMETERS FOR CASE 2					
Parameter	Value	PRODESY	F.A.S.T. CBM	GEM	ECLIPSE
Area, Ac	80	✓	✓	✓	✓
Thickness, ft	12.5	✓	✓	✓	✓
Initial Average Pressure, psia	700	✓	✓	✓	✓
Fracture porosity, %	1	✓	✓	✓	✓
Water Saturation (Fractures), %	100	✓	✓	✓	✓
Coal Density, gm/cc	1.5	✓	✓	✓	✓
Fracture Permeability, md	2	✓	✓	✓	✓
Langmuir Pressure, psia	100	✓	✓	✓	✓
Langmuir Volume, scf/ton	591	✓	✓	✓	✓
Well Bottom-hole pressure, psia	50	✓	✓	✓	✓
Fracture, half-length, ft	250	✓	✓	✓	✓
Temperature, °F	70	✓	✓	✓	✓
Sorption Time. days				250	
Diffusion Coefficient, ft^2/d					5.797 e-7
Sigma, ft^{-2}					6,900
Gas in Place, Bscf		1.055	1.055	1.055	1.055
Water in Place, STB		N/A	N/A	77,655	77,774
Cum. Gas Production @20 years, MMscf		407	412	407	407
Recovery Factor, %		38.6	39	38.6	38.6

Case 3

For case 3 (horizontal well), just one of the semi-analytical software programs (Prodesy) was included in the comparison, because the others (F.A.S.T. CBM and PROMAT) do not have the option for modeling horizontal wells. Fig. 4.4 shows half of the model geometry for this test case. Table 4.4 shows the input parameters used for this case (the check marks refers to the required input data).
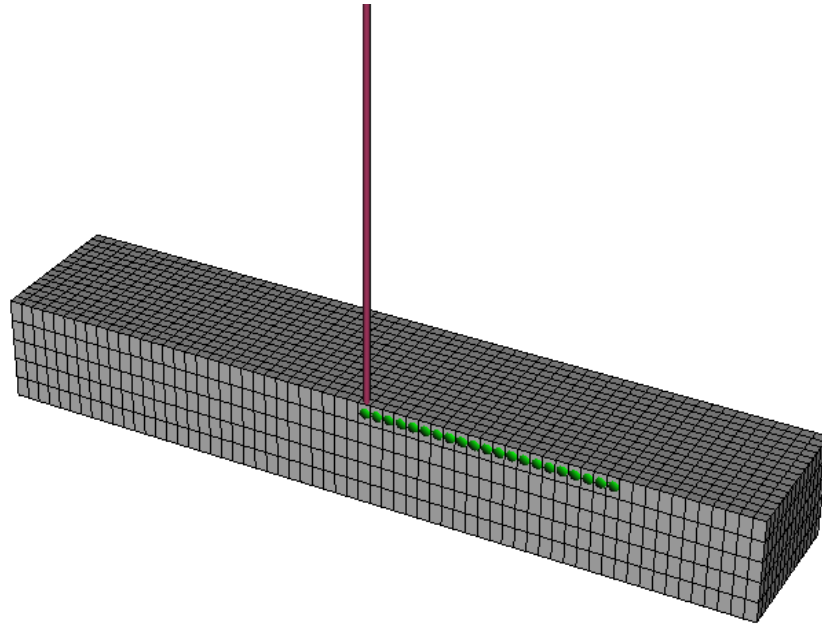
Horizontal Well

Figure. 4.4 Model Geometry Case 3 (Horizontal Well).

TABLE 4.4 RESERVOIR PARAMETERS FOR CASE 3				
Parameter	Value	PRODESY	GEM	ECLIPSE
Area, Ac	160	✓	✓	✓
Thickness, ft	7.7	✓	✓	✓
Initial Average Pressure, psia	715	✓	✓	✓
Fracture porosity, %	2	✓	✓	✓
Water Saturation (Fractures), %	100	✓	✓	✓
Coal Density, gm/cc	1.52	✓	✓	✓
Fracture Permeability, md	0.4	✓	✓	✓
Langmuir Pressure, psia	280	✓	✓	✓
Langmuir Volume, scf/ton	830	✓	✓	✓
Well Bottom-hole pressure, psia	100	✓	✓	✓
Horizontal Wellbore length, ft	1760	✓	✓	✓
Temperature, °F	70	✓	✓	✓
Sorption Time. days			46	
Diffusion Coefficient, ft^2/d				3.15 e-6
Sigma, ft^{-2}				6,900
Gas in Place, Bscf		1.5	1.5	1.5
Water in Place, STB		N/A	196,168	191,526
Cum. Gas Production @20 years, MMscf		660	343	342
Recovery Factor, %		44	22.8	22.8

Case 4

This case corresponds to a real field case for a hydraulically fractured vertical well. Table 4.5 summarizes the reservoir parameters for this real field example. To establish the impact in gas production performance by using the different formulations for shape factor and sorption time, Eqs. 3.4, 3.5, 3.6, and 3.8 were used for modeling this case. The

diffusivity coefficient was set to 3.15E-6 ft^2/d and the cleat spacing to 0.0655 ft. Applying

these parameters in Eqs. 3.4, 3.5, 3.6, and 3.8 the resulting values for sorption time are 90.8,

23, 113 and 46 days respectively.

TABLE 4.5 RESERVOIR PARAMETERS FOR CASE 4			
Parameter	Value	GEM	ECLIPSE
Area, Ac	80	✓	✓
Thickness, ft	12.5	✓	✓
Initial Average Pressure, psia	700	✓	✓
Fracture porosity, %	0.3	✓	✓
Water Saturation (Fractures), %	100	✓	✓
Coal Density, gm/cc	1.52	✓	✓
Fracture Permeability, md	0.7	✓	✓
Langmuir Pressure, psia	280	✓	✓
Langmuir Volume, scf/ton	830	✓	✓
Fracture, half-length, ft	250	✓	✓
Temperature, ℉	70	✓	✓
Diffusion Coefficient, ft^2/d			3.15 e-6
Cleat Spacing, ft	0.0655		
* Sigma, ft^{-2}			3496, 13985, 2797, 6900.
* Sorption Time. Days		90.8, 23, 113, 46.	

* Values from Equations 3.4, 3.5, 3.6 and 3.8 respectively.

Taking into account that software programs do not include diffusion for their models, only the reservoir simulators were used for modeling case 4.

Case 5

This case corresponds to a real field example for a horizontal well. Table 4.6 summarizes the reservoir parameters for this case. Taking into account that software programs do not include diffusion for their models, only the reservoir simulators were used to model case 5. To establish how the sorption time impacts in gas production performance, the different formulations for shape factor and sorption time were used for modeling this case. The diffusivity coefficient was set to 3.15E-6 ft^2/d and the cleat spacing to 0.0655 ft.

TABLE 4.6 RESERVOIR PARAMETERS FOR CASE 5			
Parameter	Value	GEM	ECLIPSE
Area, Ac	160	✓	✓
Thickness, ft	7.7	✓	✓
Initial Average Pressure, psia	715	✓	✓
Fracture porosity, %	0.03	✓	✓
Water Saturation (Fractures), %	100	✓	✓
Coal Density, gm/cc	1.52	✓	✓
Fracture Permeability, md	0.35	✓	✓
Langmuir Pressure, psia	280	✓	✓
Langmuir Volume, scf/ton	830	✓	✓
Well Bottom-hole pressure, psia	100	✓	✓
Horizontal Wellbore length, ft	3520	✓	✓
Temperature, °F	70	✓	✓
Diffusion Coefficient, ft^2/d			3.15 e-6
Cleat Spacing, ft	0.0655		
* Sigma, ft^{-2}			3496, 13985, 2797, 6900.
* Sorption Time. Days		90.8, 23, 113, 46.	

* Values from Equations 3.4, 3.5, 3.6 and 3.8 respectively.

Case 6

Also, a Multi-well case is analyzed to establish the impact in production performance by using the different approaches to sorption time. Fig. 4.5 shows the grid for modeling the multi-well case (synthetic data) which includes 10 wells (8 vertical and 2 horizontal CBM wells). Taking into account that semi-analytical software programs do not include diffusion for their models, only the reservoir simulators were used to model this case.
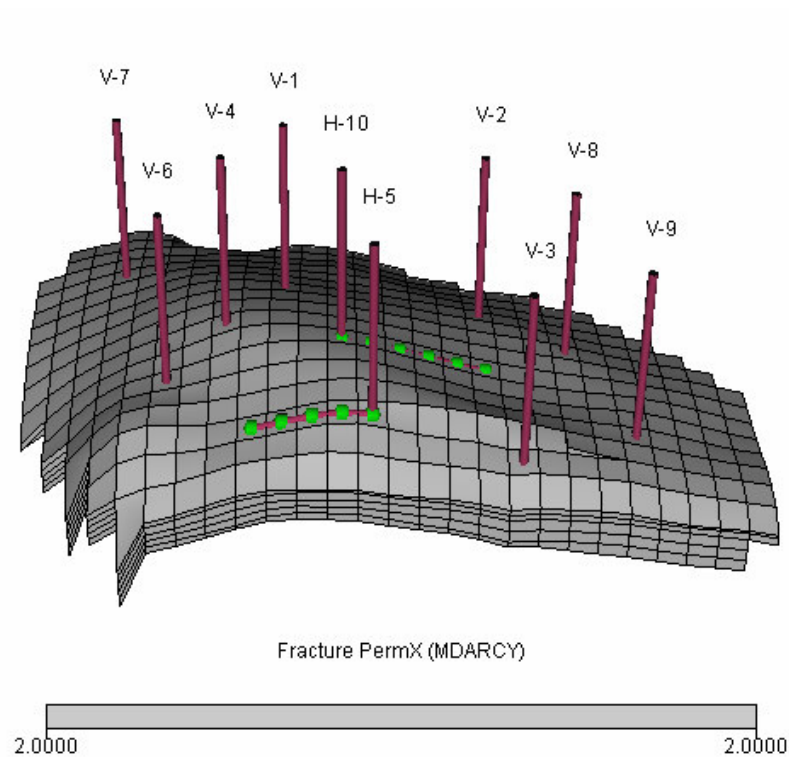

Fig. 4.5 Grid Model Geometry Case 6 (Multi-well).

For this case, fluids and rock parameters are the same as those for case 2. To establish the influence in gas production performance by using the different formulations for sorption time, Eqs. 3.3, 3.4, 3.5, 3.6, and 3.8 were used for modeling this case. The

diffusivity coefficient was set to 3.15E-6 ft^2/d and the cleat spacing to 0.0655 ft. Applying

these parameters in Eqs. 3.3, 3.4, 3.5, 3.6, and 3.8 the resulting values for sorption time are

54, 90.8, , 23, 113 and 46 days respectively.

CHAPTER V

RESULTS AND ANALYSIS

Original Gas in Place for all the test cases is consistent for all of the computation methods. The OGIP is estimated from Eq. 2.1 and Eq. 2.3.

For case 1 (single vertical well) the production profiles obtained using the several methods are shown in Fig. 5.1. For this case different trends have been noticed in the early time production behavior (when the gas peak occurs and most of the gas is produced). The response from the numerical simulators compared with the semi-analytical software programs present a higher gas peak.
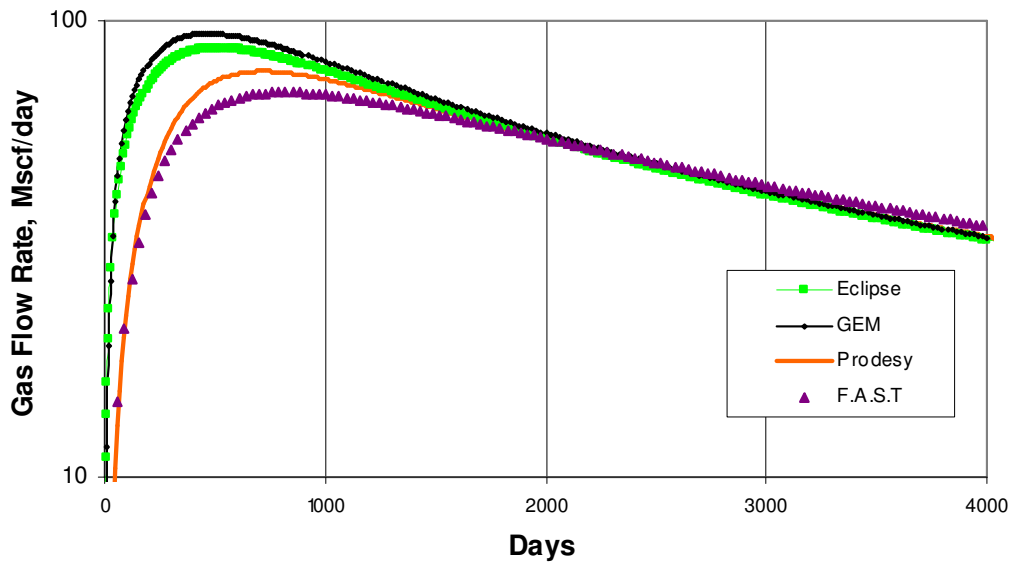

Figure. 5.1 Production Performance Results for Case 1.

For case 1b (case 1, dry coal), the results are shown in Fig. 5.2. For this case the results from the different computation methods are similar. However, it is important to mention that for obtaining this match the sorption time in the reservoir simulators was set to 1 day (instantaneous desorption). This was the only case which it was run the software PROMAT.
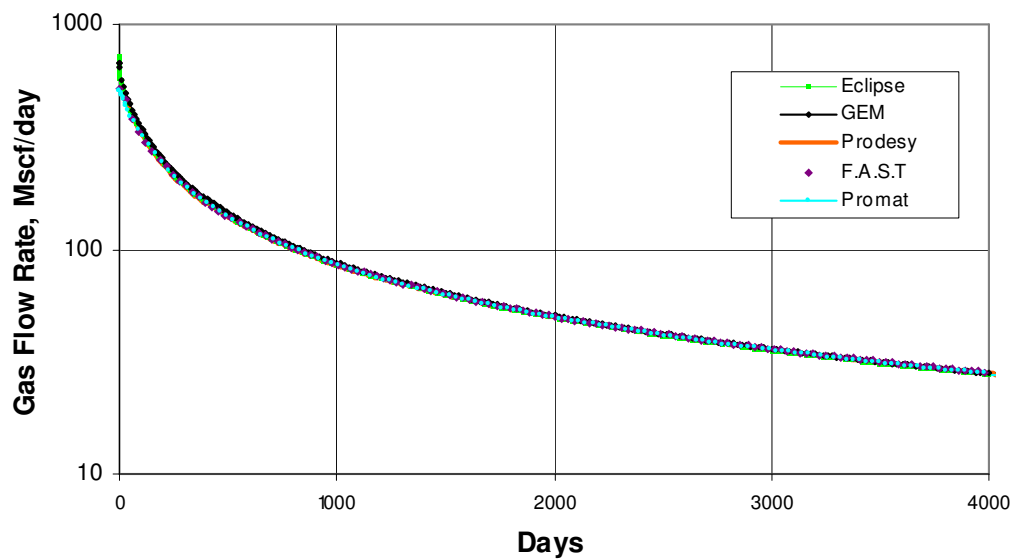

Figure. 5.2 Production Performance Results for Case 1b.

For case 2 (vertical fractured well) the production profiles obtained using the several methods are shown in Fig. 5.3. For this case the results from the reservoir simulators (Eclipse and GEM) are consistent with each other. The response from the semi-analytical software programs compared with simulators presents the gas flow rate curve shifted to the right.
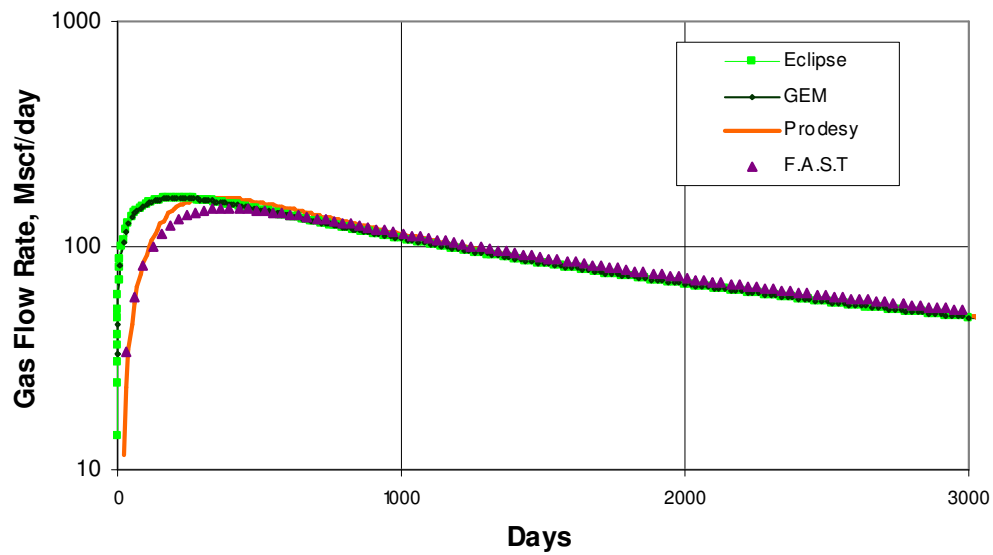
Figure. 5.3 Production Performance Results for Case 2.

For case 2b (case 2, dry coal), the results are shown in Fig. 5.4. For this case the results from the different computation methods exhibit the same trend (for this match sorption time in the reservoir simulators was set to 1 day).
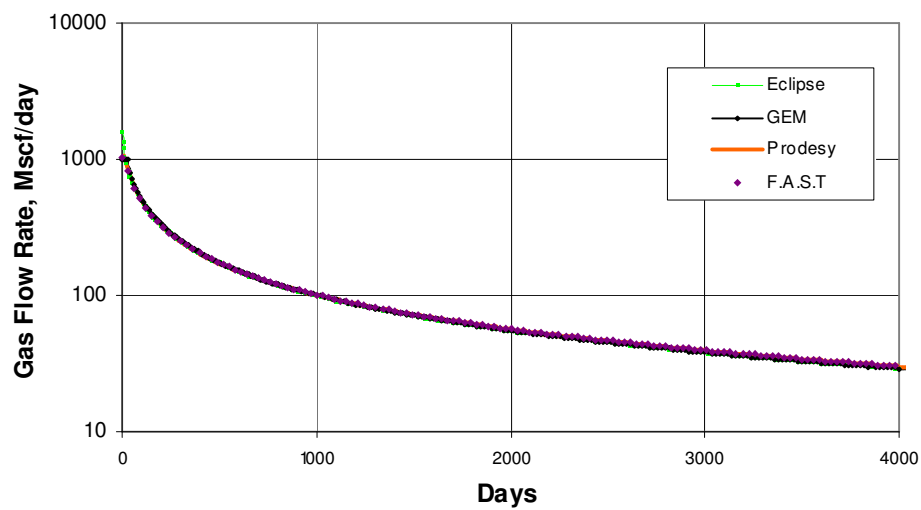

Figure. 5.4 Production Performance Results for Case 2b.

For case 3 (horizontal well) the production profiles obtained using the several methods are shown in Fig. 5.5. For case 3, the production profile from Prodesy presents important differences when compared with simulators. Neither F.A.S.T. CBM nor PROMAT have the option for modeling horizontal wells.
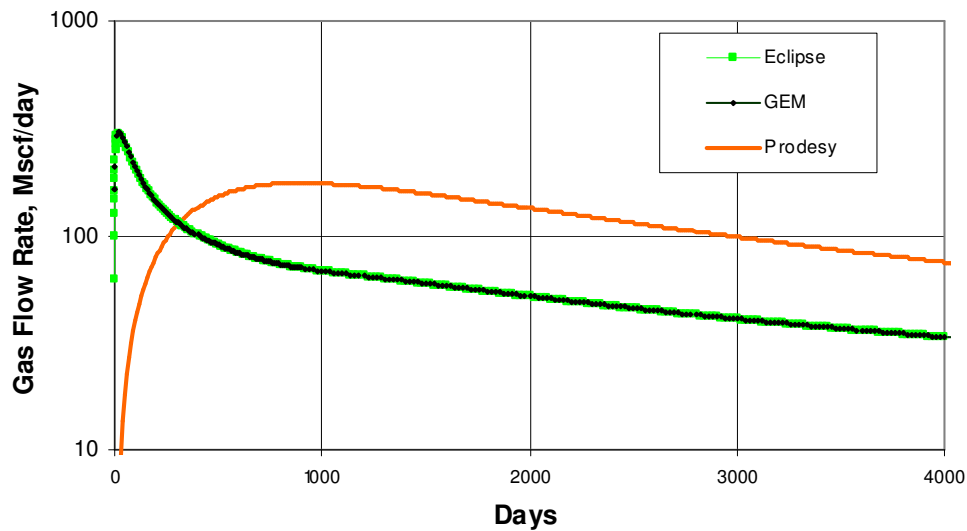

Figure. 5.5 Production Performance Results for Case 3.

For case 3b (case 3, dry coal), the results are shown in Fig. 5.6. For this case, the production profile from Prodesy presents important differences when compared with simulators response (for this match sorption time in the reservoir simulators was set to 1 day).
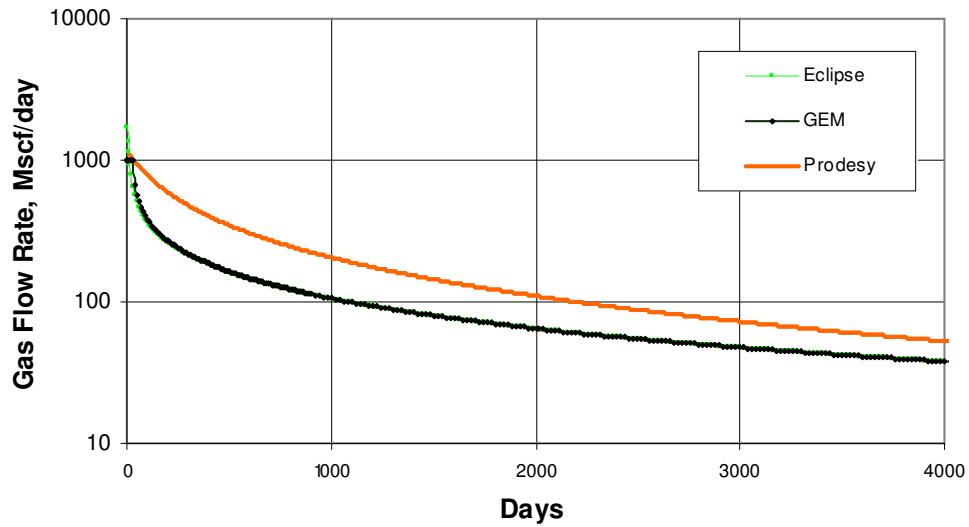
Figure. 5.6 Production Performance Results for Case 3b.

For cases 1, 2, and 3, the production performance response from the reservoir simulators (Eclipse and GEM) seem consistent with each other.

Figs. 5.7, 5.8, 5.9, and 5.10 show the simulation results for case 4 comparing the different formulations for sorption time and the match with the real production data.

Figure. 5.7 Production Performance Results for Case 4 (τ from Equation 3.4).

Figure. 5.8 Production Performance Results for Case 4 (τ from Equation 3.5).
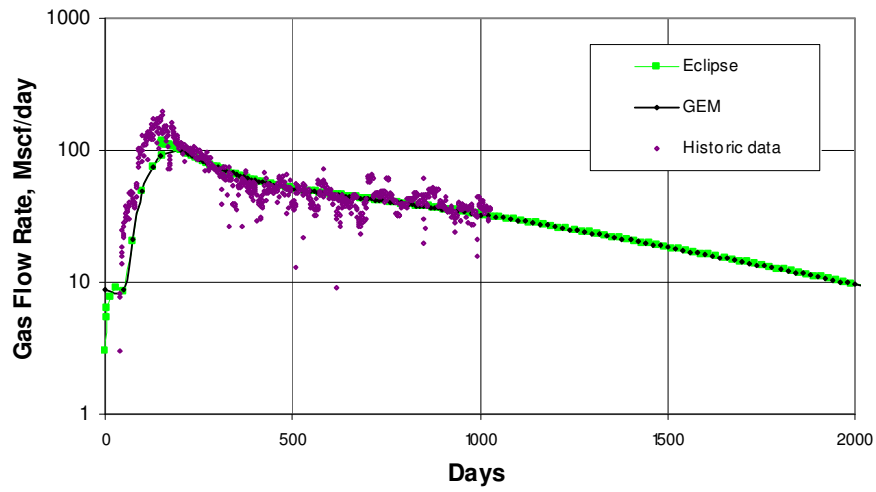
Figure. 5.9 Production Performance Results for Case 4 (τ from Equation 3.6).
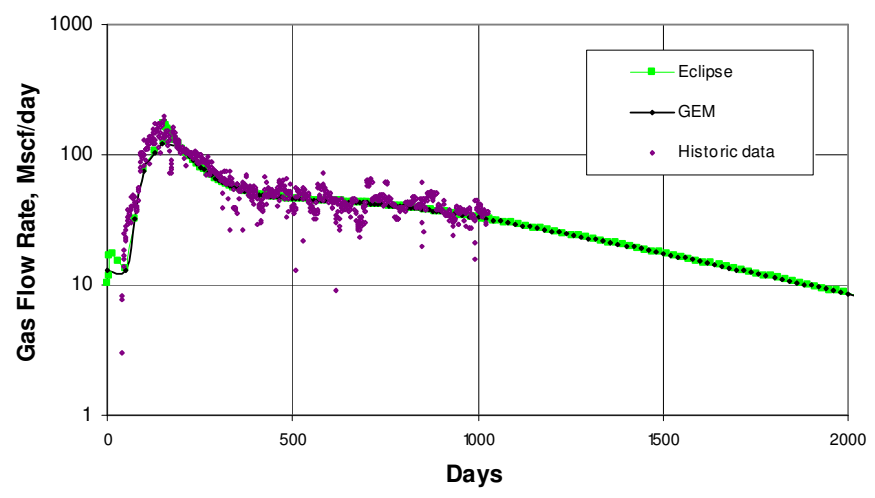
Figure. 5.10 Production Performance Results for Case 4 (τ from Equation 3.8).

Figs. 5.11, 5.12, 5.13, and 5.14 show the simulation results for case 5 comparing the different formulations for sorption time and the match with the real production data.

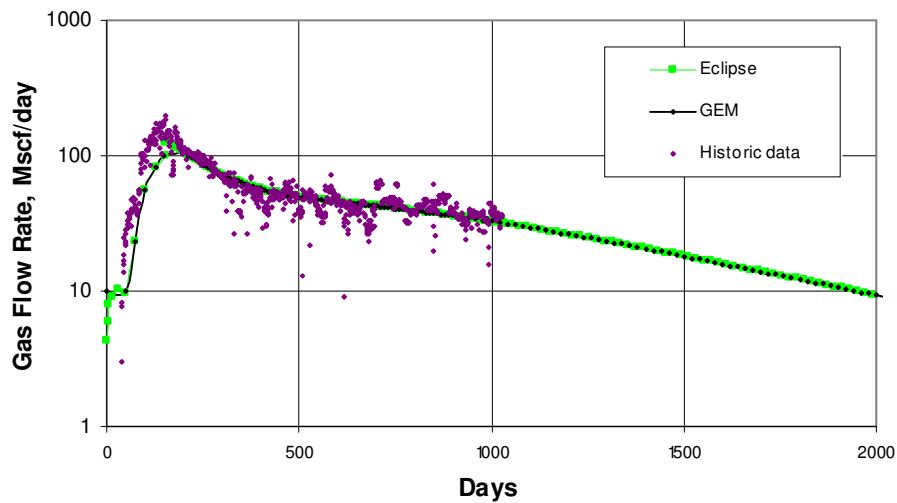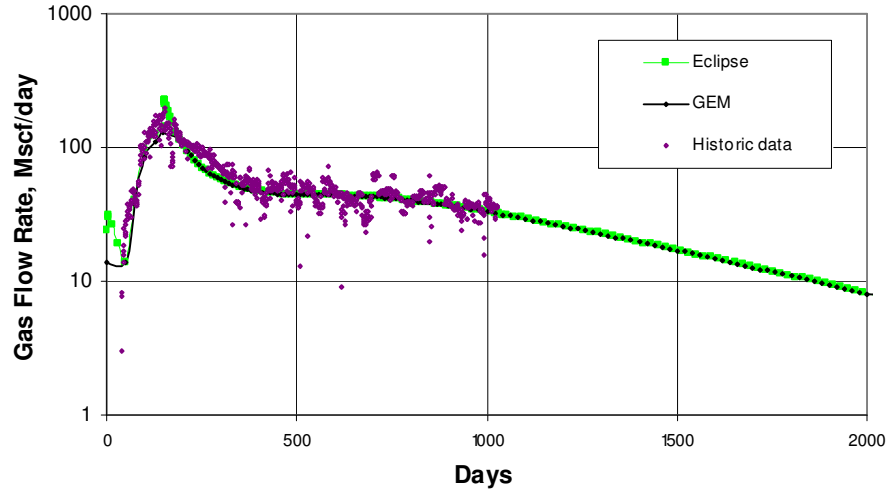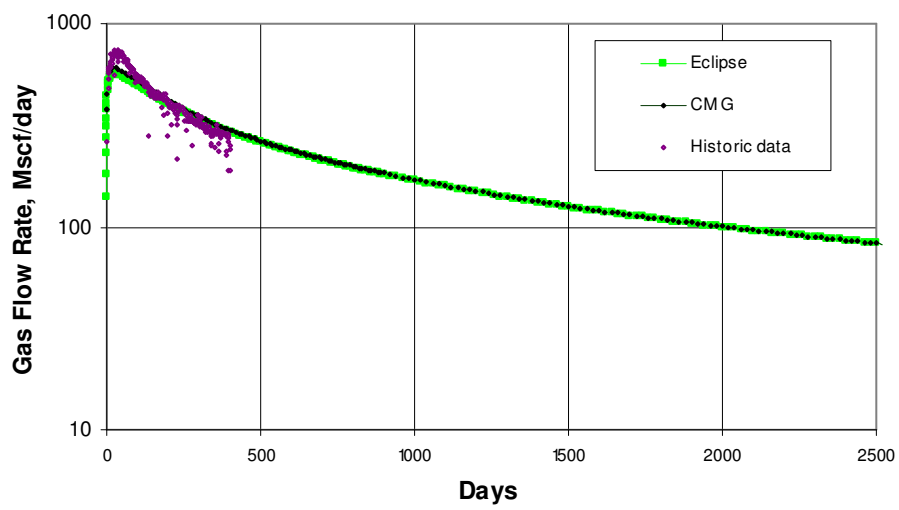**Figure. 5.11 Production Performance Results for Case 5 (τ from Equation 3.4).**
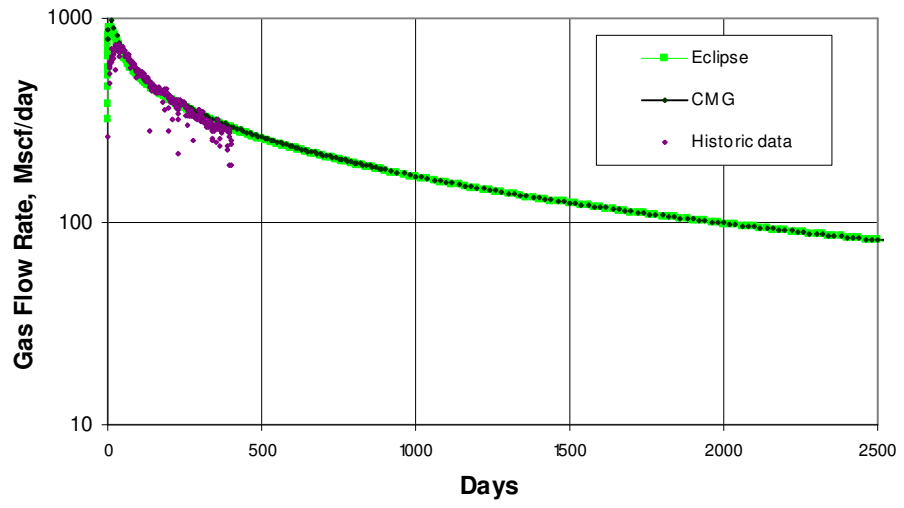
Figure. 5.12 Production Performance Results for Case 5 (τ from Equation 3.5).
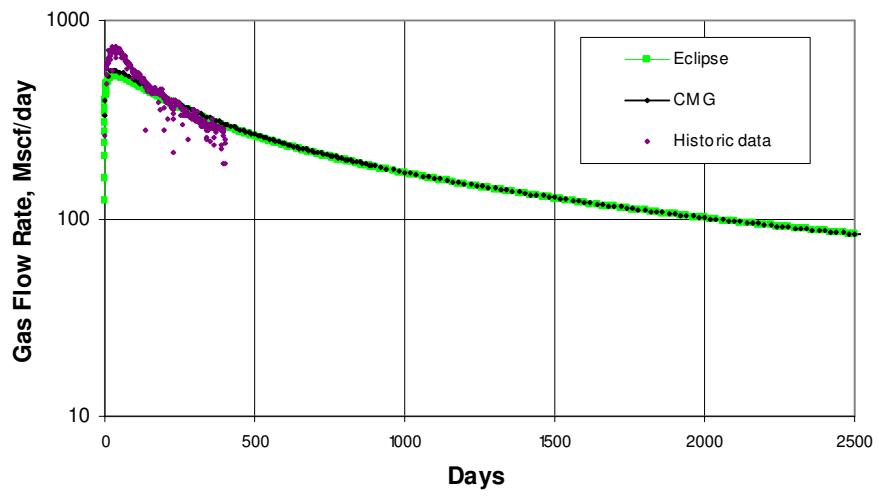
Figure. 5.13 Production Performance Results for Case 5 (τ from Equation 3.6).
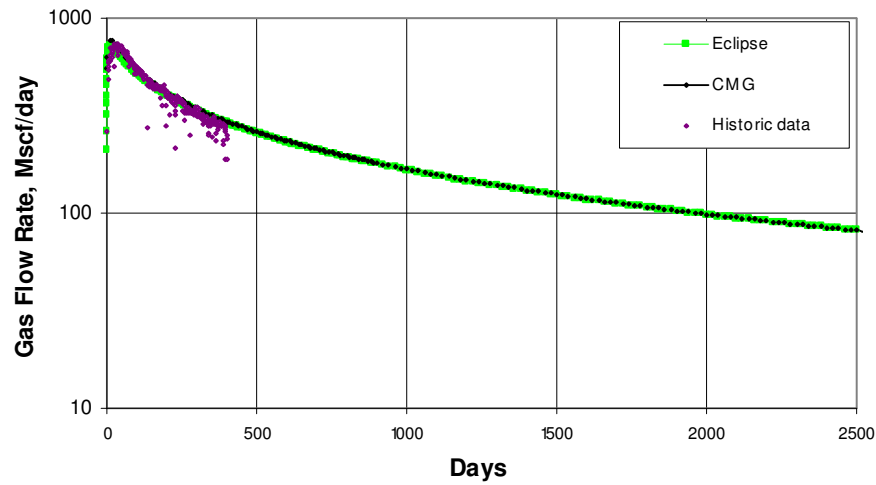
Figure. 5.14 Production Performance Results for Case 5 (τ from Equation 3.8).

According to the results from cases 4 and 5, using Eq. 3.8 to estimate sorption time and modeling the diffusion process in the simulators, the best match is obtained with the actual production data. By applying the erroneous formulation for τ, an incorrect gas peak estimation for CBM wells is obtained.

Fig. 5.15 shows the different production performance results from case 6 for the total field (multi-well case) using the different approaches to shape factor and sorption time.
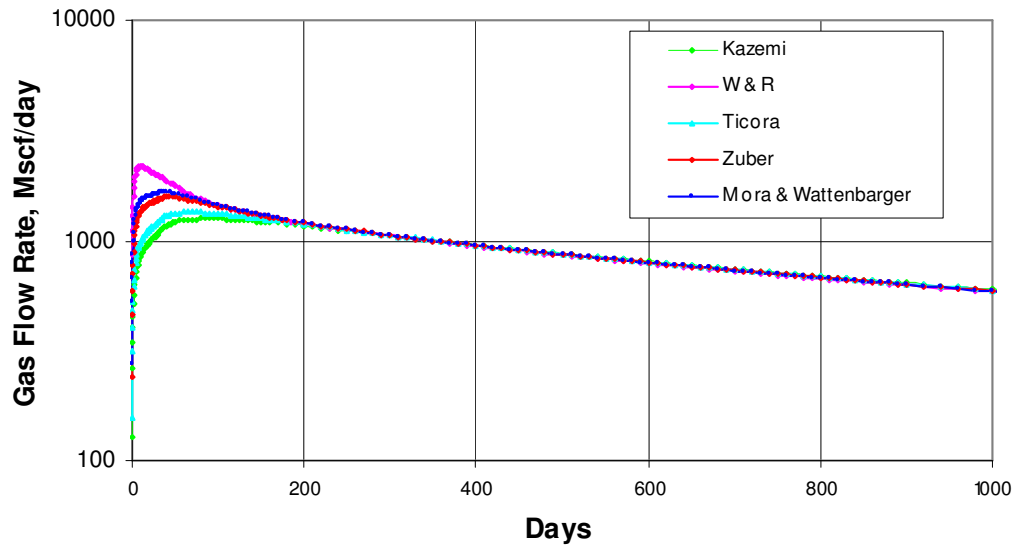
Figure. 5.15 Production Performance Results for Case 6.

Fig. 5.16 shows the comparison results from case 6 (assuming a drilling program of 1 well per month.) using the different formulations for shape factor and sorption time.
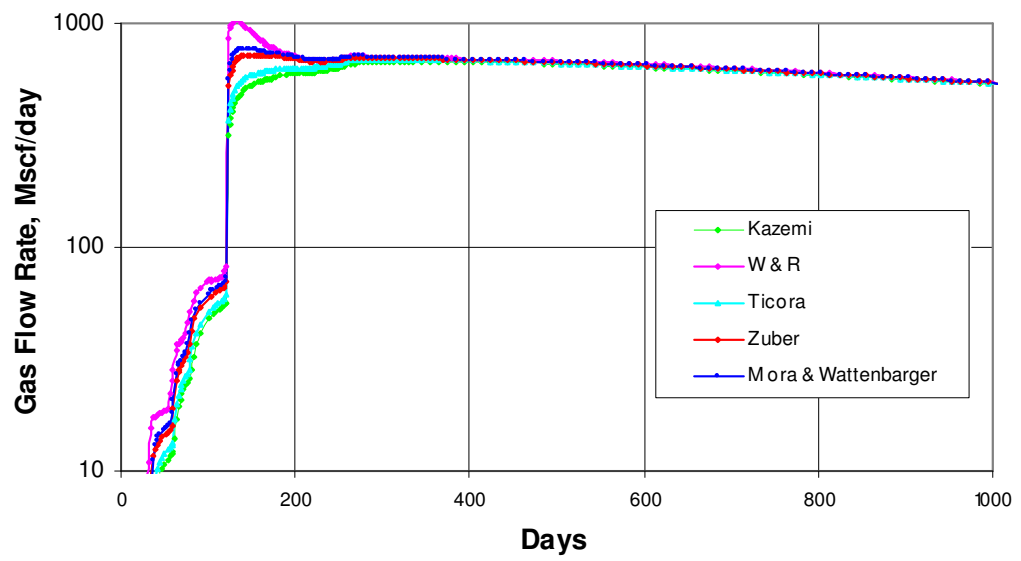
Figure. 5.16 Production Performance Results for Case 6 (Drilling Program 1 Well/month).

The late time production behavior seems to be consistent for the different test cases and computation methods. However, the early production behavior (when the gas peak occurs and most of the gas is produced) exhibit important differences which can affect the project economics.

For the different computation methods and cases, the water production performance was about the same. As mentioned before, the flow in cleat system is governed by Darcy's Law.

CHAPTER VI

CONCLUSIONS

The following conclusions are based on the results obtained in this research.

The numerical reservoir simulators include diffusion (Fick's Law) for modeling CBM reservoirs, but semi-analytical software programs do not include diffusion. The semi-analytic models combine desorption (Langmuir Isotherm) and equations for conventional reservoirs.

Production performance from both numerical reservoir simulators (Eclipse and GEM) were about the same. However, to be consistent, special care has to be taken with the input for the diffusion parameters in each simulator.

When comparing the production performance between simulators and programs, different production profiles have been identified. The results show that in the early production behavior (when the gas peak occurs and most of the gas is produced) important differences exist between programs and simulators.

For dry coal, the results from the different computation methods exhibit the same trend when instantaneous desorption is assumed in reservoir simulators (except for the horizontal well case).

Shape Factors, σ, are used for both Dual Porosity and CBM reservoir models. For CBM reservoirs, shape factor, sorption time, and the diffusivity coefficient are closely related for modeling diffusion process.

Several authors have presented different formulas to estimate shape factor for dual porosity models, leading to considerable confusion. It was found that some of the most popular formulas do not seem to be correct. The correct formulas for shape factors are shown have been verified..

Shape factors value and formulas from this study are consistent with certain previous studies for stabilized constant pressure drainage and when the boundary condition is constant rate (pseudo-steady state).

It is not clear whether constant fracture pressure or pseudo-steady state formulas should be used, but constant fracture pressure is usually preferred. Both are presented in this study.

For real field examples the best match to the real production profile was obtained when the correct formula for shape factor (Eq. 3.8) was applied to estimate sorption time, τ.

The formulas for shape factor and sorption time suggested in this study can be used not only for production performance prediction but also for history matching studies.

By applying erroneous formulation for σ, and τ, an incorrect production performance and gas peak estimation for CBM wells are obtained.

NOMENCLATURE

A	=	area, acres
B	=	formation volume factor, rb/stb
c	=	matrix concentration, scf/rcf
c_f	=	fracture concentration, scf/rcf
c_t	=	total compressibility, psi^{-1}
D	=	diameter, ft
D_c	=	diffusion coefficient, ft^2/day
G_c	=	Initial Gas content, scf/ton
h	=	Thickness, ft
k_m	=	matrix permeability, md
k_f	=	fracture permeability, md
L	=	fracture spacing
L_x	=	fracture spacing in x direction
L_y	=	fracture spacing in y direction
L_z	=	fracture spacing in z direction
n	=	sets of normal parallel fractures
p_m	=	average matrix pressure, psia
p_f	=	fracture pressure, psia
p_L	=	Langmuir pressure, psia
q_g	=	Gas Production rate, scf/day
q_w	=	Water Production rate, STB/day

q^* = matrix-fracture drainage rate, rcf/day/rcf

r = radius, ft

r_w = wellbore radius, ft

S_w = Water saturation, fraction

t_D = dimensionless time based on r^2

V_b = matrix block volume, rcf

V_L = Langmuir volume, scf/ton

x_f = half-length fracture, ft

Z^* = gas compressibility factor for unconventional reservoirs, dimensionless

Greek Letters

ϕ = porosity, fraction

λ = interporosity flow coefficient, dimensionles

μ = viscosity, cp

ρ_b = coal density, gm/cc

σ = shape factor, ft^{-2}

τ = sorption time, hours

ω = storativity ratio, fraction

REFERENCES

1. Warren, J.E., and Root, P.J.: "The Behavior of Naturally Fractured Reservoirs," *SPEJ* (September 1963) **22**, 245-255.

2. Zuber, M.D. *et al*.: "The Use of Simulation and History Matching To Determine Critical Coalbed Methane Reservoir Properties," paper SPE/DOE 16420 presented at the 1987 SPE/DOE Low Permeability Reservoir Symposium, Denver, 18-19 May.

3. Seidle, J.P., and Arri, L.E.: "Use of Conventional Reservoir Models for Coalbed Methane Simulation," paper CIM-90/SPE 21599 presented at the 1990 International Technical Meeting, Calgary, 10-13 June.

4. King, G.R.: "Material Balance Techniques for Coal Seam and Devonian Shale Gas Reservoirs," paper SPE 20730 presented at the 1990 Annual Technical Conference and Exhibition, New Orleans, 23-26 September.

5. Seidle J.P.: "A Modified p/z Method for Coal Wells," paper SPE 55605 presented at the 1999 Rocky Mountain Regional Meeting, Gillette, Wyoming, 15–18 May.

6. Jensen, D and Smith, L.K.: "A Practical Approach to Coalbed Methane Reserve Prediction Using a Modified Material Balance Technique", International Coalbed Methane Symposium, Tusaloosa, Alabama, May 1997.

7. David, H. and Law, S.: "Numerical Simulator Comparison Study for Enhanced Coalbed Methane Recovery Processes, Part I: Carbon Dioxide Injection," paper SPE 75669 presented at the 2002 SPE Technology Symposium, Calgary, 30 April-2 May.

8. Hower, T.L.: "Coalbed Methane Reservoir Simulation: An Envolving Science," paper SPE 84424 presented at the 2003 SPE Annual Technical Conference and Exhibition, Denver, 5-8 October.

9. Jalal, J. and Shahab, D.M.: "A Coalbed Methane Reservoir Simulator Designed for the Independent Producers," paper SPE 91414 presented at the 2004 SPE Eastern Regional Meeting, Charleston, West Virginia, 15-17 September.

10. Aminian, K. *et al*.: "Type Curves for Coalbed Methane Production Prediction," paper SPE 91482 presented at the 2004 SPE Eastern Regional Meeting, Charleston, West Virginia, 15-17 September.

11. ECLIPSE Technical Description Manual; "Coalbed Methane Model", Schlumberger, (2005).

12. CBM Technical Manual, Fekete & Associates, Calgary (2006).

13. Kazemi, H.: "Numerical Simulation of Water-Oil Flow in Naturally Fractured Reservoirs" *SPEJ* (December 1976) 317-326.

14. Mora, C.A., Wattenbarger, R.A.: "Analysis and Verification of Dual Porosity and CBM Shape Factors," paper CIPC 2006-139 presented at the 2006 Petroleum Society Canadian International Petroleum Conference, Calgary, 13-15 June.

15. Reservoir Assessment Report Analysis Submitted to El Paso Production Company, Ticora Geo., Arvada, Colorado, (August 2004).

16. Barenblatt, G.I. *et al*.: "Basic Concepts in the Theory of Seepage of Homogeneous Liquids in Fissured Rocks," *Soviet Applied Mathematics and Mechanics*, (June 1960) **24**, 852-864.

17. Lim, K.T., Aziz, K.: "Matrix Fracture Transfer Shape Factors for Dual Porosity Simulators". *Journal of Petroleum Science and Engineering* (November 1994) **13**, 169-178.

18. Coats, K. H.: "Implicit Compositional Simulation of Single-Porosity and Dual-Porosity Reservoirs," SPE 18427 presented at the 1989 Symposium of Reservoir Simulation, Houston, 6-8 February.

19. Zimmerman, R.W. *et al*.: "A Numerical Dual-Porosity Model with Semianlytical Treatment of Fracture/matrix Flow," *Water Resources Research* (1993) **29**, 2127-2137.

20. Carslaw, H.S., Jaeger, J.C.: *Conduction of Heat in Solids*, Second Edition, Oxford Science Publications, New York City (1959).

APPENDIX A

CBM AND DUAL POROSITY SHAPE FACTORS

A naturally fractured reservoir is characterized as a system of matrix blocks with each matrix block surrounded by fractures. The fluid drains from the matrix block into the fracture system which is interconnected and leads to the well. Warren and Root[1] introduced a mathematical model for this dual porosity matrix/fracture behavior.

Their model has been widely used for many types of reservoirs, including tight gas and coalbed methane reservoirs. A key part of their model is a geometrical parameter (shape factor) which controls drainage rate from matrix to fractures. Although Warren and Root gave formulas for calculating shape factors, many other authors have presented alternate formulas, leading to considerable confusion.

In addition to the size and shape of a matrix element, two cases are considered by authors: constant drainage rate from a matrix block and constant pressure in the adjacent fractures.

The current work confirmed the correct formulas for shape factors by using numerical simulation for the various cases. It was found that some of the most popular formulas do not seem to be correct.

Naturally fractured reservoirs can be characterized as a system of fractures in a very low conductivity rock. The mathematical formulation of this "dual porosity" or "double porosity" system of matrix blocks and fractures was presented by Barenblatt, *et al* [16]. The first system is a fracture system with low storage capacity and high fluid transmissibility and the second system is the matrix system with high storage capacity and low fluid transmissibility. The matrix rock stores almost all of the fluid but has such low

conductivity, that fluid just drains from the matrix "block" into adjacent fractures as is shown in Fig. A.1. The fractures have relatively high conductivity but very little storage. q^* is the flow rate divided by the matrix volume. Either p_f or q^* is constant for these cases.

$$p_f$$

$$p_f \qquad \begin{array}{c} p_m \\ \textbf{(matrix pressure)} \end{array} \qquad p_f$$

$$p_f$$
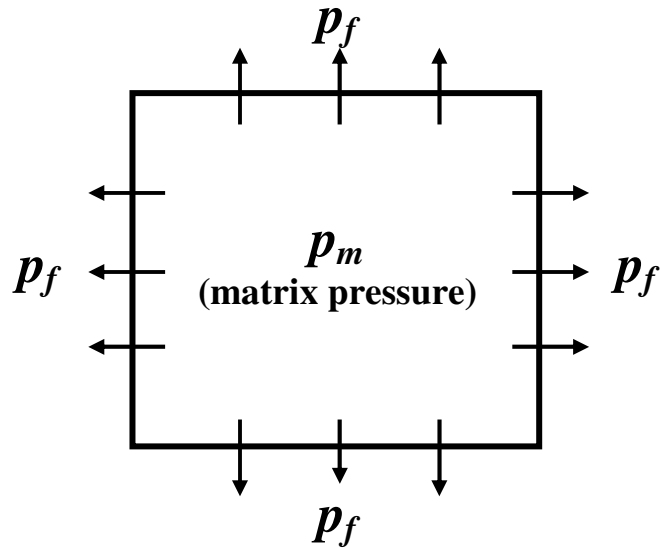
Figure. A.1 Sketch of Flow Rate from Matrix to Fractures (Difference Between p_m and p_f).

The drainage from matrix to fractures for dual porosity reservoirs was idealized by Warren and Root[1] according to Eq. A.1.

$$q^* = \sigma \frac{k_m}{\mu} \left(p_m - p_f \right) \qquad \text{…………….……………………………...……} \qquad \text{A.1}$$

Eq. A.1 is in the form of pseudo-steady state flow which means that early transient effects have been ignored. Pseudo-steady state also means that the drainage rate is constant. The units of Eq. A.1 are volume rate of fluid drainage per volume of reservoir. The units of the shape factor, σ, are $1/L^2$.

For dual porosity reservoirs, when pseudo-steady state production test analysis are available, the product $\sigma \cdot k_m$ can be determined using Eq. A.2, but can not be separated.

$$\sigma\, k_m = \frac{\lambda\, k_f}{r_w^2} \quad \dots\dots\dots\dots\dots\dots\dots\dots\dots\dots\dots\dots\dots\dots\dots\dots\dots\dots\dots\dots\dots\dots \quad \text{A.2}$$

When k_m is available from core or log analysis, then shape factor, σ can be estimated. For cases where Pressure Test Analysis are not available, formulas can be used to estimate shape factor. However, there are conflicting equations and values for σ in literature.

Many authors have interpreted Eq. A.1 to be the equivalent long term drainage equation with p_f held constant and drainage rate changing with time. In that case, σ has a different value than for the constant rate case. So, σ depends on the size and shape of a matrix block and also on the boundary condition assumed at the matrix/fracture interface.

The flow mechanics of coalbed methane (CBM) production have some similarities to the dual porosity system. CBM models are characterized as a coal/cleat system of equations. Most of the gas is stored in the coal blocks. Gas desorbs in the coal block and then drains to the fracture system by molecular diffusion (Fick's Law rather than Darcy's Law). The drainage rate from the coal block can be expressed using Eq. A.3.

$$q^* = \sigma \cdot D_c \cdot (\bar{c} - c_f) \quad \dots\dots\dots\dots\dots\dots\dots\dots\dots\dots\dots\dots\dots\dots\dots\dots\dots\dots\dots \quad \text{A.3}$$

For both equations A.1 and A.3, q^* represents drainage rate per volume of reservoir. When these mathematical expressions (dual porosity and CBM drainage rate) are compared, these equations look similar and both of them use shape factor, σ.

Shape Factor Values and Formulas

Matrix-fracture drainage shape factor formulas have been presented by a number of authors. Many of them are different, leaving confusion about which formulas are correct. Here it is presented a brief summary of existing formulas for σ.

Warren and Root[1] presented an analytical solution for dual porosity models, based on the mathematical concepts introduced by Barenblatt *et al* [16]. According to Warren and Root and their idealization of the heterogeneous porous medium, the fractures are the boundaries of the matrix blocks. The Warren and Root[1] approach for "shape factor" assume uniformly spaced fractures and allow variations in the fracture width to satisfy the conditions of anisotropy, according to Eq. A.4.

$$\sigma = \frac{4n(n+2)}{L^2}$$ ……….…………….…………………………………...…… A.4

According to Eq. A.4, L is spacing between fractures and n is one, two or three parallel sets of fractures and it is associated with different flow geometries (slabs, rectangular columns and cubes respectively). Substituting values for n, and assuming equal spacing between fractures, $L_x=L_y=L_z=L$, σ is equal to $12/L^2$, $32/L^2$, and $60/L^2$ for one, two and three sets of normal parallel fractures respectively.

Perhaps the most widely used formula for σ was presented by Kazemi[13]. It was developed by finite difference methods for a three dimensional numerical simulator for fractured reservoirs. Kazemi's formula (Eq. A.5) is currently used by commercial reservoir simulators for dual porosity and CBM models.

$$\sigma = 4\left(\frac{1}{L_x^2} + \frac{1}{L_y^2} + \frac{1}{L_z^2}\right)$$ …………………………….……….………...…… A.5

According to this equation, for equal fracture spacing, σ has a value of $4/L^2$, $8/L^2$ and $12/L^2$ for one, two and three sets of fractures respectively. The value for three sets of fractures compares to Warren & Root's but for different flow geometry (1 set of fractures). They cannot both be right. In addition, there are a number of other formulas that have been presented by different authors. An excellent review of some of these formulas was presented by Lim & Aziz[17].

Coats[18] derived values for σ under pseudo-steady sate condition (constant rate). These values are equal to $12/L^2$, $28.45/L^2$, and $49.58/L^2$ for one, two and three sets of normal parallel fractures respectively.

Zimmerman[19] presented a different approach for σ values using different flow geometries with constant-pressure boundary conditions.

Lim & Aziz[17] presented analytical solutions of pressure diffusion draining into a constant fracture pressure (boundary condition). From Lim & Aziz study was derived a general equation for shape factor (Eq. A.6).

$$\sigma = \pi^2 \left(\frac{1}{L_x^2} + \frac{1}{L_y^2} + \frac{1}{L_z^2} \right) \dots\dots\dots\dots\dots\dots\dots\dots\dots\dots\dots\dots\dots\dots\dots\dots \quad \text{A.6}$$

For equal fracture spacing, σ is equal to $3\pi^2/L^2$ for three sets of fractures. For one and two sets of fractures the values for σ are π^2/L^2 and $2\pi^2/L^2$, respectively. Also solutions for cylindrical and spherical flow geometry were presented considering constant boundary pressure. For these geometries σ has a value of $18.17/L^2$ and $25.67/L^2$, respectively. The shape factor values derived by Lim and Aziz[17] are consistent with Zimmerman's [19].

Experimentation and Results

Numerical simulation was used for obtaining shape factor values under pseudo-steady state conditions. Two different reservoir simulators were used for this study, Gassim a single phase 1D-2D simulator and Eclipse a multiphase 3D commercial reservoir simulator.

To simulate matrix-fracture drainage, a single matrix grid with fractures as boundaries was assumed. High permeability and low porosity are associated to the fracture system (boundaries) and the opposite for the matrix system. The "fracture" was either specified as constant pressure or constant rate.

Slab Geometry (one parallel set of fractures)

For the case with one set of fractures (slab geometry), fractures were considered just in "*x*" direction and the fracture spacing is given by the slab thickness (*L*). Matrix-fracture flow has been simulated as a single matrix problem with one fracture as a boundary (dual porosity or CBM system) as is shown in Fig. A.2.
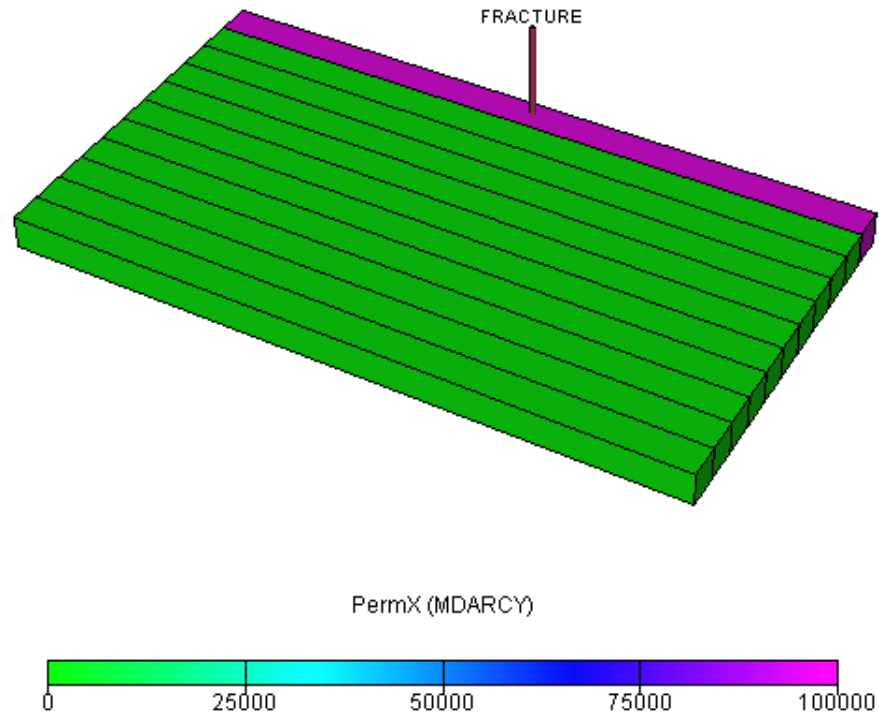
Figure. A.2 Grid for Modeling Slab Geometry.

The model in Fig. A.2 represents half of the slab and according to the grid geometry high permeability and low porosity define the fracture system (boundary) and the opposite for the matrix system. Matrix-Fracture flow was simulated for two boundary conditions (draining in constant pressure and draining in constant rate). Fig. A.3 shows the pressure difference due to the flow from matrix to fracture.
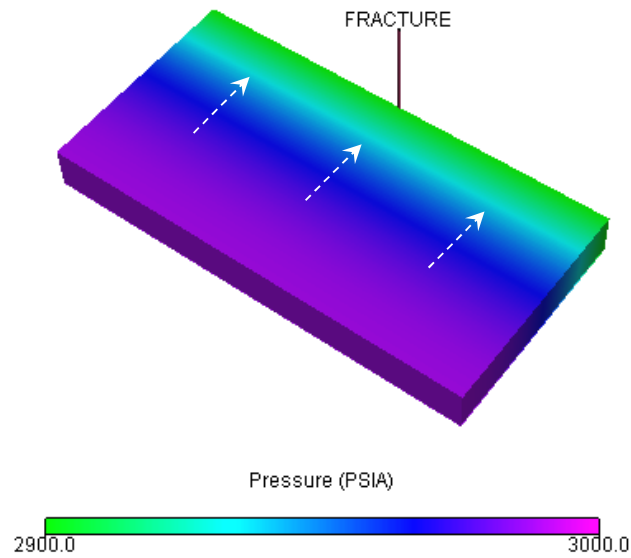
Figure. A.3 Pressure Change for Matrix-facture Flow (Slab Geometry).

Table A.1 shows a summary of the parameters used for modeling the simulation cases.

TABLE A.1 SUMMARY OF PARAMETERS FOR SIMULATION CASES	
k_m, md	0.1
μ, cp	0.7
B, rb/stb	1
h, ft	20
a, ft	40
b, ft	40

The parameters a and b belong to the dimensions of the matrix system in x and y direction respectively.

Flow from matrix to fractures was simulated under two boundary conditions (draining in constant pressure and draining in constant rate). The simulation values of pressure under stabilized flow (Fig. A.4), and the parameters from Table A.1 were used to calculate the shape factor value.
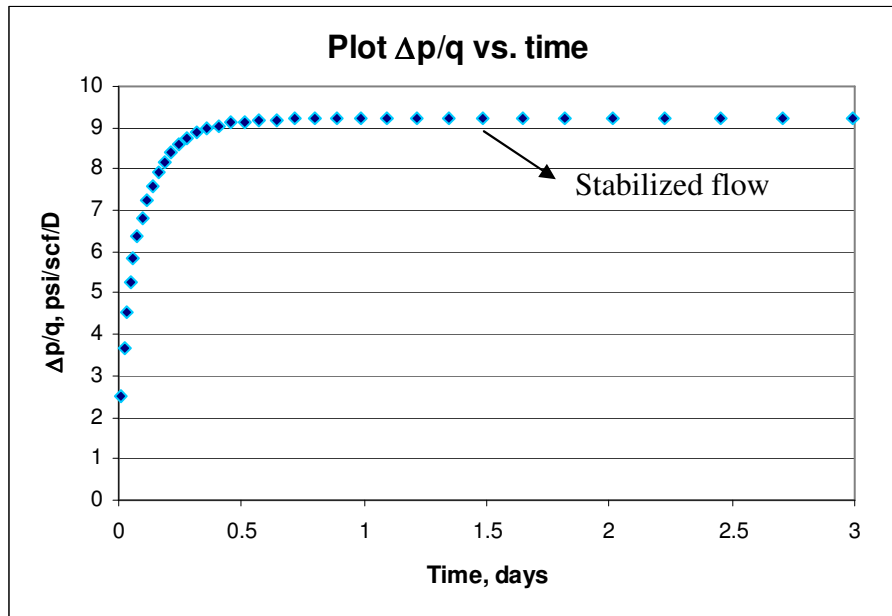

Figure. A.4 Delta p / q from Simulation for the Slab Geometry under Constant Rate.

For obtaining shape factor values, Eq. A.1 was reordered and solved as Eq. A.7.

$$\sigma = \frac{\mu \cdot q}{k_m \cdot (p_m - p_f) \cdot V_b}$$ …….…………………….…………………………………...…….   A.7

For this case the matrix volume corresponds to the product *(a∗b∗h = 32,000 ft³)*. For the constant rate case, the value Δp/q under stabilized flow from Fig. A.4 is equal to *9.2.* Because the simulation model represents half of slab the value for Δp/q used in Eq. A.7 was

(9.2/2 = 4.6). Solving the equation the value for σ was estimated as 0.007497. For this case

the fracture spacing, *L,* is 40 ft. So, the value for shape factor in terms of fracture spacing is

$0.007497*L^2$ = $12/L^2$. Same procedure was used to estimate shape factor for all the

geometries for each boundary condition.

According to the simulation results, σ has a value of π^2/L^2 when the boundary

conditions is constant pressure, however σ has a value of *$12/L^2$* when the boundary condition

is constant rate. Comparing the results from both simulators (Gassim and Eclipse),

consistent values have been obtained for σ under the two boundary conditions.

Columns Geometry (two parallel sets of fractures)

For this case the grid geometry considers fractures in "*x*" and "*y*" directions and the

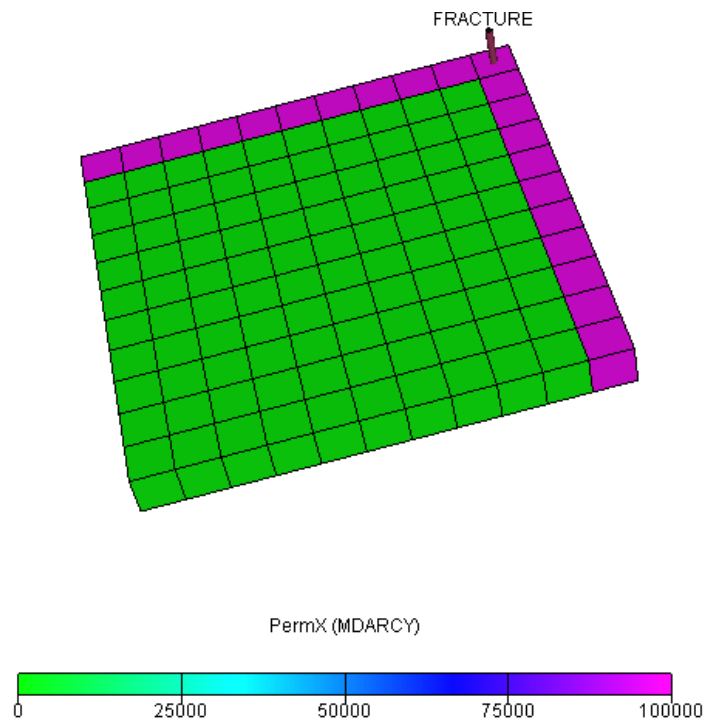fracture spacing is given by L_x and L_y as is shown in Fig. A.5.

Figure. A.5 Grid for Modeling Columns Geometry.

The model represents one quarter of column and the distance between fractures in x and y direction is the same. High permeability and low porosity are associated to the fractures (boundaries) and the opposite for the matrix. Fig. A.6 shows the pressure difference due to the flow from matrix to the fractures in both directions.
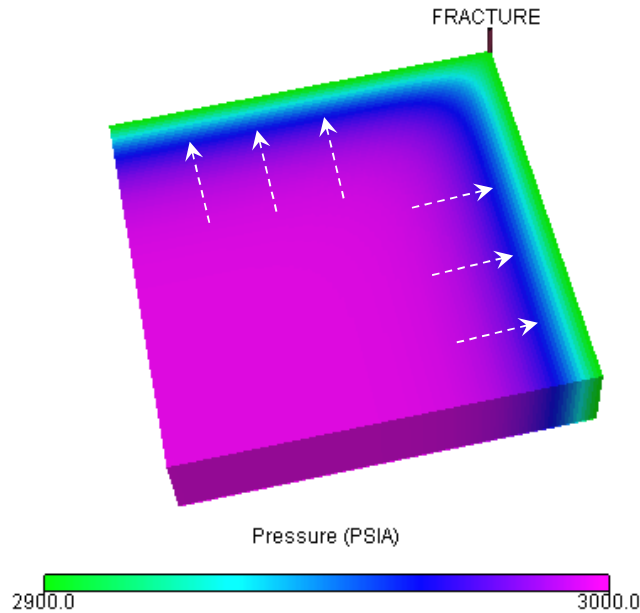

FRACTURE

Pressure (PSIA)

2900.0   3000.0

Figure. A.6 Pressure Change for Matrix-facture Flow (Columns Geometry).

Following same procedure used for slab case, and according to the simulation results, σ for columns case has a value of $2\pi^2/L^2$ when the boundary condition is constant pressure, however σ has a value of $28.43/L^2$ when the boundary condition is constant rate. Consistent σ values have been obtained from both simulators. Fig. 2 shows the grid model used to simulate columns geometry.

Cubes Geometry (three parallel sets of fractures)

Grid geometry for this case considered fractures in "*x*", "*y*" and "*z*" directions and the fracture spacing is given by L_x, L_y and L_z as is shown in Fig. A.7.
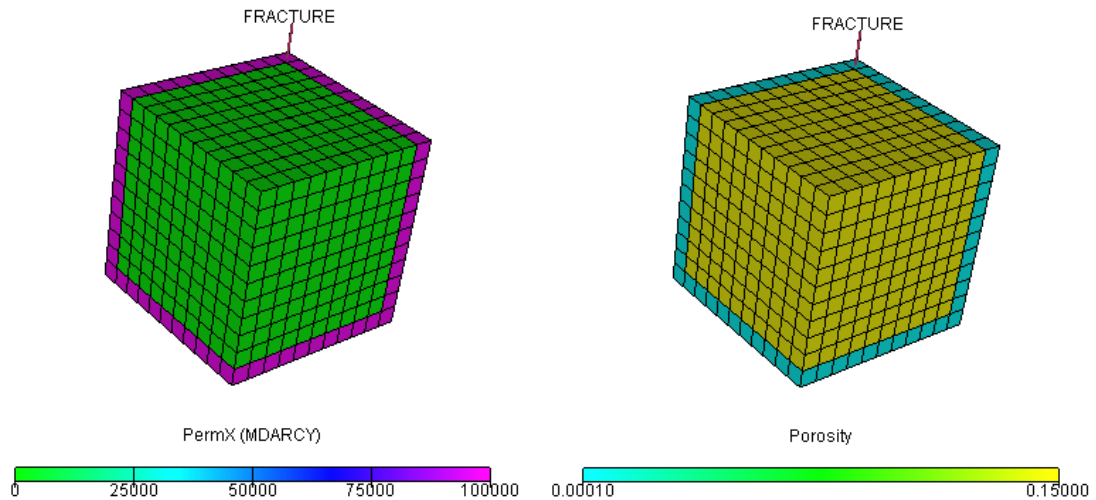

Figure. A.7 Grid for Modeling Cubes Geometry.

The model represents *1/8* of cub, and the distance between fractures in *x, y* and *z was* fixed equal. Permeability and porosity contrasts between matrix and fractures (boundaries) are presented same way as it was presented for the cases before. Fig. A.8 shows the pressure difference due to the flow from matrix to the fractures in the three directions.
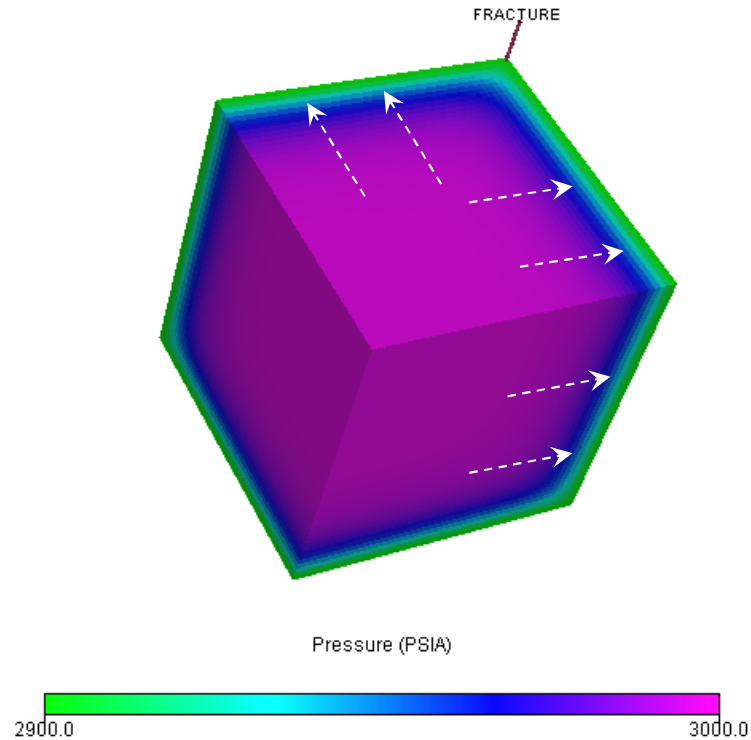
Figure. A.8 Pressure Change for Matrix-facture Flow (Cubes Geometry).

For this case, σ has been evaluated as $3\pi^2/L^2$ when the boundary conditions is constant pressure and σ has been evaluated as $49.48/L^2$ when the boundary condition is constant rate.

Cylindrical Geometry (Radial Case)

This flow geometry was simulated just for comparing with Zimmerman and Lim & Aziz calculations but this case does not represent a real petroleum engineering problem. The grid geometry considers matrix flow from the center to the outer boundary (fracture) as is shown in Fig. A.9. High permeability and low porosity are associated to the fracture (outer boundary) and the opposite for the matrix. Fig. A.10 shows the pressure difference due to matrix-fracture drainage.

FRACTURE

PERMR

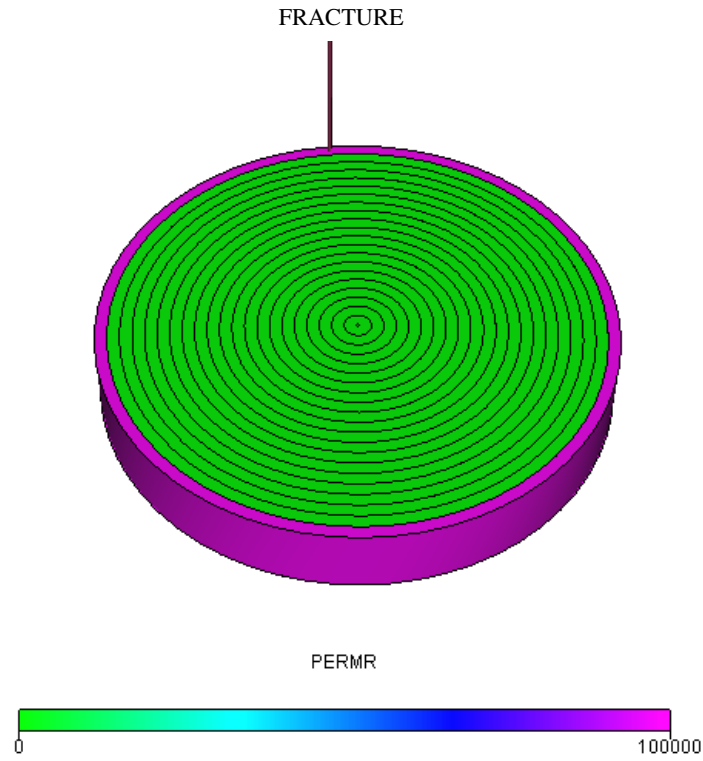0   100000

Figure. A.9 Grid for Modeling Cylindrical Geometry.

FRACTURE

Pressure (PSIA)

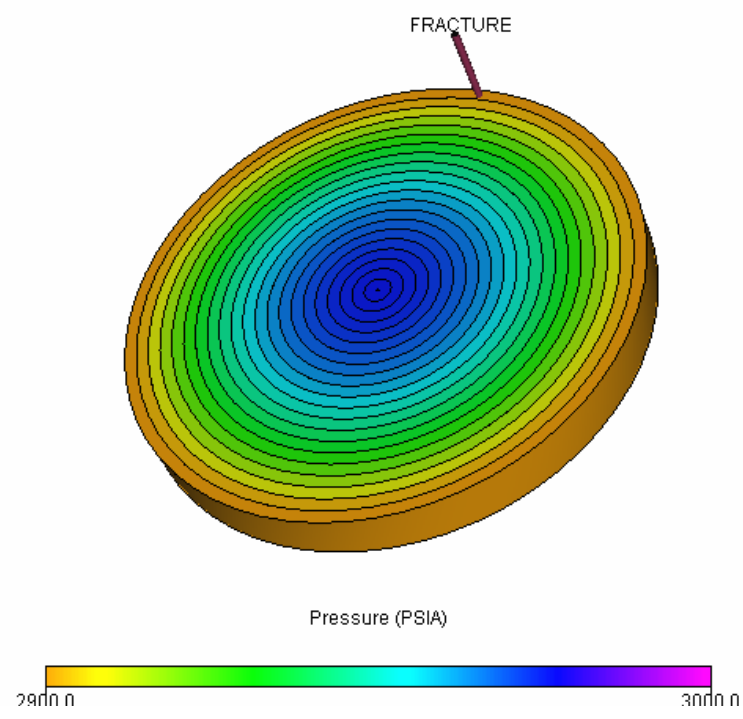2900.0   3000.0

Figure. A.10 Pressure Change for Matrix-facture Flow (Cylindrical Geometry).

According to the simulation results, σ has a value of $23.11/D^2=18.17/L^2$ when the boundary condition is constant pressure, and when the boundary condition is constant rate σ has a value of $32/D^2=25.13/L^2$. The results were obtained in terms of diameter (D) but for comparison purposes the values also are presented in terms of L using equivalent areas.

Spherical Geometry

This geometry was not able to be analyzed using numerical simulation. However analytical solutions were used for obtaining shape factor values.

The bases for the analytical solutions were taken from Carslaw & Jaeger[20] and converted to flow in a porous medium.

Constant pressure case: For a solid sphere with initial pressure $= p_i$ and the outer pressure held at p_f, Carslaw & Jaeger[20] show:

$$(p_i - p_m) = (p_i - p_f)(1 - \frac{6}{\pi^2} \sum_{n=1}^{\infty} \frac{1}{n^2} e^{-n^2 \pi^2 t_D})$$

This can then be differentiated and put into the form

$$q = V_b \phi c_t (p_i - p_f) \frac{6k}{\phi \mu c_t r^2} \sum_{n=1}^{\infty} e^{-n^2 \pi^2 t_D}$$

Taking only the first term for the long-term solution gives

$$\frac{q}{V_b} = \frac{\pi^2}{r^2} \frac{k}{\mu} (p_m - p_f)$$

Using Eq. A.7 for the definition of shape factor, then

$$\sigma = \frac{\pi^2}{r^2} = \frac{4\pi^2}{D^2}$$

Constant rate case: For a solid sphere with initial pressure $= p_i$ and flow rate from the outer radius held constant (ignoring the decay term for a long term solution) Carslaw & Jaeger[20] show:

$$(p_i - p_f) = \frac{q}{4 \pi r^2} \left[\frac{3t}{\phi c_t r} + \frac{(2r^2)}{10 k / \mu r} \right]$$

And using the pressure depletion expression for constant rate production,

$$p_i - p_m = \frac{q}{V_b \phi c_t} t \ ,$$

and substituting this into the previous equation, then we have

$$\frac{q}{V_b} = \frac{15}{r^2} \frac{k}{\mu} (p_m - p_f)$$

So, the shape factor for constant rate drainage is

$$\sigma = \frac{15}{r^2} = \frac{60}{D^2}$$

So, with this analytical solution, σ has a value of $4\pi^2/D^2 = 25.67/L^2$ when the boundary condition is constant pressure, and when the boundary condition is constant rate σ has a value of $60/D^2 = 38.98/L^2$.

As it was shown before, the σ values for cylindrical and spherical geometries when the boundary condition is constant rate ($32/D^2$ and $60/D^2$ respectively) look similar to values presented for Warren and Root[1] for 2 and 3 sets of fractures.

General Equation for Shape Factor

In order to obtain general equations for shape factor, when fracture spacing changes with direction, parallelepiped geometry was considered.
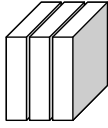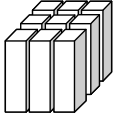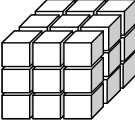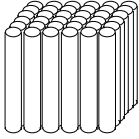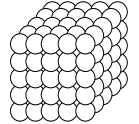
According to the results, the general formulation for shape factor given by Lim & Aziz[17], when the boundary condition is constant pressure, was confirmed as is presented in Eq. A.8.

$$\sigma = \pi^2 \left(\frac{1}{L_x^{\,2}} + \frac{1}{L_y^{\,2}} + \frac{1}{L_z^{\,2}} \right) \quad \dots\dots\dots\dots\dots\dots\dots\dots\dots\dots\dots\dots\dots\dots\dots\dots\dots\dots \quad \text{A.8}$$

Also an empirical equation for shape factor has been derived from this study when the boundary condition is constant rate. Eq. A.9 can be written as follows:

$$\sigma = \frac{2.31 \cdot n^2 + 9.5 \cdot n + 0.19}{n} \left(\frac{1}{L_x^{\,2}} + \frac{1}{L_y^{\,2}} + \frac{1}{L_z^{\,2}} \right) \quad \dots\dots\dots\dots\dots\dots\dots\dots\dots\dots\dots\dots\dots \quad \text{A.9}$$

Where *n* represents the number of normal sets of fractures (*1, 2* or *3*). Tables A.2 and A.3 present a comparison of shape factor values from this study and previous published studies.

TABLE A.2 SHAPE FACTOR VALUES FROM DIFFERENT AUTHORS $(\sigma \cdot L^2)$						
			Constant Fracture Pressure		*Constant Rate (pss)*	
Geometry	W & R[1]	Kazemi[13]	Zimmerman[19] / Lim & Aziz[17]	This Study	Coats[18]	This Study
	12	*4*[*]	$\pi^2 = 9.87$	$\pi^2 = 9.87$	*12*	*12*
	32[**]	*8*[*]	$2\pi^2 = 19.74$	$2\pi^2 = 19.74$	*28.5*	*28.43*
	60[**]	*12*[*]	$3\pi^2 = 29.61$	$3\pi^2 = 29.61$	*49.6*	*49.48*
			$18.17\left(= L^2\,\dfrac{23.11}{D^2}\right)$	$18.17\left(= L^2\,\dfrac{23.11}{D^2}\right)$		$25.13\left(= L^2 \cdot \dfrac{32}{D^2}\right)$
			$25.67\left(= L^2\,\dfrac{4\pi^2}{D^2}\right)$	$25.67\left(= L^2\,\dfrac{4\pi^2}{D^2}\right)$		$38.98\left(= L^2 \cdot \dfrac{60}{D^2}\right)$

[*] Erroneous values
[**] Misunderstanding values

TABLE A.3 SUMMARY OF RECOMMENDED SHAPE FACTOR VALUES

	1 D Slabs	2 D Columns	3 D Cubes / Parallelpipeds	Cylinder	Sphere
Constant Pressure	$\sigma = \dfrac{\pi^2}{L^2} = \dfrac{9.87}{L^2}$	$\sigma = \dfrac{\pi^2}{\bar{k}}\left(\dfrac{k_x}{L_x^2} + \dfrac{k_y}{L_y^2}\right)$ *For Isotropic:* $\sigma = \pi^2\left(\dfrac{1}{L_x^2} + \dfrac{1}{L_y^2}\right)$ *When $L_x = L_y = L_z$* $\sigma = \pi^2\left(\dfrac{1}{L_x^2} + \dfrac{1}{L_x^2}\right)$ $\sigma = \dfrac{2\pi^2}{L^2} = \dfrac{19.74}{L^2}$	$\sigma = \dfrac{\pi^2}{\bar{k}}\left(\dfrac{k_x}{L_x^2} + \dfrac{k_y}{L_y^2} + \dfrac{k_z}{L_z^2}\right)$ *For Isotropic:* $\sigma = \pi^2\left(\dfrac{1}{L_x^2} + \dfrac{1}{L_y^2} + \dfrac{1}{L_z^2}\right)$ *When $L_x = L_y = L_z$* $\sigma = \pi^2\left(\dfrac{1}{L_x^2} + \dfrac{1}{L_x^2} + \dfrac{1}{L_x^2}\right)$ $\sigma = \dfrac{3\pi^2}{L^2} = \dfrac{29.61}{L^2}$	$\dfrac{23.11}{D^2} = \dfrac{18.17}{L^2}$	$\dfrac{4\pi^2}{D^2} = \dfrac{25.67}{L^2}$
Constant Rate	$\sigma = \dfrac{12}{L^2}$	$\sigma = \dfrac{14.215}{\bar{k}}\left(\dfrac{k_x}{L_x^2} + \dfrac{k_y}{L_y^2}\right)$ *For Isotropic:* $\sigma = 14.215\left(\dfrac{1}{L_x^2} + \dfrac{1}{L_y^2}\right)$ *When $L_x = L_y = L_z$* $\sigma = 14.215\left(\dfrac{1}{L_x^2} + \dfrac{1}{L_x^2}\right)$ $\sigma = \dfrac{28.43}{L^2}$	$\sigma = \dfrac{16.493}{\bar{k}}\left(\dfrac{k_x}{L_x^2} + \dfrac{k_y}{L_y^2} + \dfrac{k_z}{L_z^2}\right)$ *For Isotropic:* $\sigma = 16.493\left(\dfrac{1}{L_x^2} + \dfrac{1}{L_y^2} + \dfrac{1}{L_z^2}\right)$ *When $L_x = L_y = L_z$* $\sigma = 16.493\left(\dfrac{1}{L_x^2} + \dfrac{1}{L_x^2} + \dfrac{1}{L_x^2}\right)$ $\sigma = \dfrac{49.48}{L^2}$	$\dfrac{32}{D^2} = \dfrac{25.13}{L^2}$	$\dfrac{60}{D^2} = \dfrac{38.98}{L^2}$

The analysis in this study showed that boundary conditions (constant rate or constant boundary pressure) yield different values for σ.

For draining to constant pressure σ values presented in previous studies[17, 19] were confirmed, and also values for σ from this study are consistent with values presented by Coats[18] when the boundary condition is constant rate.

For each case (slabs, columns, cubes, and cylinder) the simulation results were also used to plot the pressure difference versus the square root of time as is shown in Fig. A.11 to estimate the time of end of the early linear.
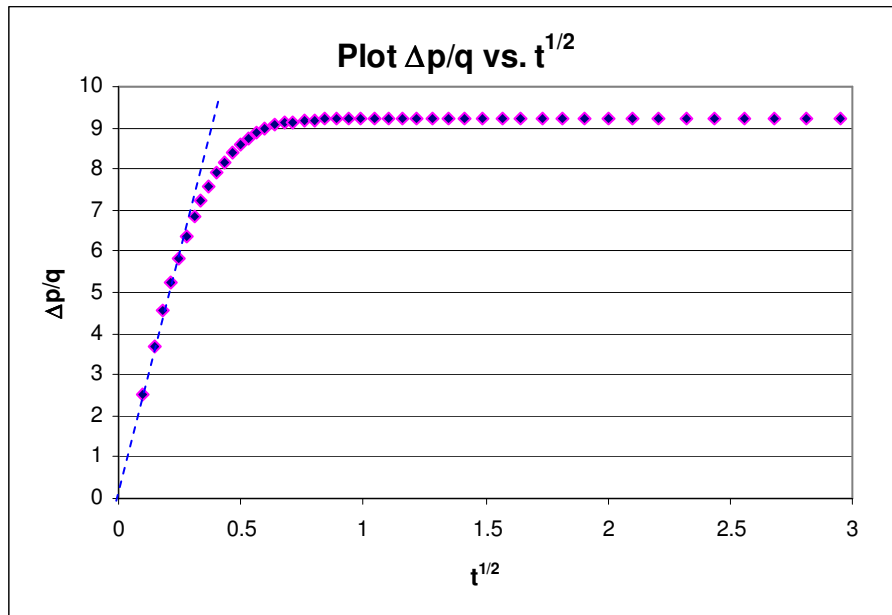
Figure. A.11 Time of End of Early Linear.

Table A.4 shows the time of end of the early linear for each case.

TABLE A.4 TIME OF END OF EARLY LINEAR		
Geometry	Constant rate	Constant pressure
slabs	0.046 days	0.061 days
columns	0.033 days	0.046 days
cubes	0.033 days	0.033 days
cylinder	0.036 days	0.054 days

APPENDIX B

DERIVATIONS FOR CBM/FICK'S LAW RELATING SHAPE FACTOR, TAU, AND DIFFUSIVITY

Stabilized Flow equation:

$$-\frac{dc}{dt} = \sigma \cdot D_c \cdot (\bar{c} - c_f) = \frac{1}{\tau} \cdot (\bar{c} - c_f) \quad , \ scf/D$$

$$-\frac{d\bar{c}}{\bar{c} - c_f} = \frac{1}{\tau} dt$$

$$ln\ (\bar{c} - c_f)\Big|_0^c = \frac{1}{\tau} \cdot t\Big|_0^t$$

$$ln\frac{\bar{c} - c_f}{\bar{c}_i - c_f} = \frac{1}{\tau} \cdot t$$

@ $t = \tau$

$$\bar{c} - c_f = (\bar{c}_i - c_f)e^{-\frac{1}{\tau} \cdot t}$$

$$\frac{\bar{c} - c_f}{\bar{c}_i - c_f} = e^{-1} = 0.3679$$

So, 63.2% of the mass has been drained (draining @ constant boundary concentration c_f)

Fluid flow (Stabilized flow equation):

$$q^* = \sigma \frac{k_m}{\mu}\left(p_m - p_f\right) \quad , \ rcf/D$$

$$\frac{q\beta}{V_m} = \sigma \frac{k_m}{\mu}\left(p_m - p_f\right)$$

$$\frac{d\overline{p}_m}{dt} = -\frac{q\beta}{V_p \cdot c_t} \quad ; \qquad \frac{rcf/D}{rcf(1/psi)} = psi/D$$

$$q = \sigma \frac{k_m}{\mu} \frac{V_m}{B}(p_m - p_f)$$

$$t = \frac{1}{(\sigma \dfrac{k_m}{\mu} \dfrac{V_m}{V_p \cdot c_t})} = \tau = \frac{1}{\sigma}\left(\frac{k_m}{\phi_m \cdot \mu \cdot c_t}\right)$$

$$\frac{dq}{q} = -\sigma \frac{k_m}{\mu} \frac{V_m}{V_p \cdot c_t} dt$$

$$ln\,q\Big|_{qi}^{q} \frac{dq}{q} = -\sigma \frac{k_m}{\mu} \frac{V_m}{V_p \cdot c_t} t\Big|_{0}^{t} \quad ; \qquad -q = q_i \cdot e^{-(\sigma \frac{k_m}{\mu} \frac{V_m}{V_p \cdot c_t}) \cdot t}$$

$$t = \frac{1}{(\sigma \dfrac{k_m}{\mu} \dfrac{V_m}{V_p \cdot c_t})} = \tau = \frac{1}{\sigma}\left(\frac{k_m}{\phi_m \cdot \mu \cdot c_t}\right) \quad \longleftarrow \text{Matrix Diffusivity}$$

$$\frac{q}{q_i} = e^{-1} = 0.3679 \qquad @\ t = \tau$$

So, q is 63.2% of q_i @ $t = \tau$

Ultimate drainage

$$c = -\frac{1}{V}\frac{dV}{dp_t}$$

For $c = $ constant:

$$\frac{dV}{V} = c \cdot dp \quad ; \qquad ln\,V\Big|_{Vi}^{V} = c \cdot p\Big|_{pi}^{p}$$

$$V = V_i \cdot e^{-c(p-p_i)}$$

$$q \cdot dt = \frac{1}{B \cdot \tau}(p_m - p_f) \cdot dt$$

$$q = q_i \cdot e^{-\frac{1}{\tau}t}$$

$$q = q_i \cdot e^{-\infty} = 0$$

$$Q \;=\; \int_0^t q \cdot dt \;=\; \int_0^t q_i \cdot e^{-\frac{1}{\tau}t} \, dt \;=\; q_i \left(-\tau \int_0^t e^{-\frac{1}{\tau}t} \, dt \right)$$

$$Q = -\tau \cdot q_i \cdot e^{-\frac{1}{\tau}t} \bigg|_0^t \;=\; -\tau \cdot q_i (e^{-\frac{1}{\tau}t} - 1)$$

$$Q_{(t=\infty)} = -\tau \cdot q_i (0 - 1) = \tau \cdot q_i$$

$$Q_{(t=\tau)} = -\tau \cdot q_i (e^{-1} - 1) = \tau \cdot q_i (1 - 0.3679) = 0.632 \cdot \tau \cdot q_i$$

$$\frac{Q_{(t=\tau)}}{Q_{(t=\infty)}} = 0.632 \qquad \text{Assuming } c = \text{constant (oil) and small (i.e. } B = B_i)$$

$$\text{So,} \quad \tau = \frac{1}{\sigma \left(\dfrac{k_m}{\phi \cdot \mu \cdot c_t}\right)_m} = \frac{1}{\sigma \cdot D_m}$$

APPENDIX C

SENSITIVITY TO LAMBDA AND OMEGA FOR DUAL POROSITY MODELS

For Naturally Fractured Reservoirs (N.F.R), the characterization models use the same parameters used for homogeneous reservoirs and two more parameters. These two parameters are Omega (ω) and Lambda (λ).

Omega, ω, is defined as the storability ratio. This parameter determines the volume of fluid stored in the fracture system compared to the total fluid in the porous system of the reservoir (matrix and fractures). The relation of ω to the reservoir parameters is given by:

$$\omega = \frac{(\phi c_t)_f}{(\phi c_t)_f + (\phi c_t)_m} \quad \text{..} \quad \text{C.1}$$

According to this formula "the higher value of ω, the higher width of the fractures". Omega, ω, represents how much fluid is stored in the fracture system compared to the total fluid in the reservoir (matrix and fractures).

Lambda, λ, is defined as the interporosity flow coefficient which determines the inter-relation between matrix blocks and the fracture system.

$$\lambda = \sigma \frac{k_m}{k_f} r_w^2 \quad \text{..} \quad \text{C.2}$$

According to this equation, λ controls how fast the fluid drains from the matrix to the fractures. The expression for Lambda includes the shape factor, σ.

The parameters Lambda and Omega are usually calculated from pressure transient analysis. For these analysis, the typical type curve for a naturally fractured reservoir is shown in Fig. C.1.
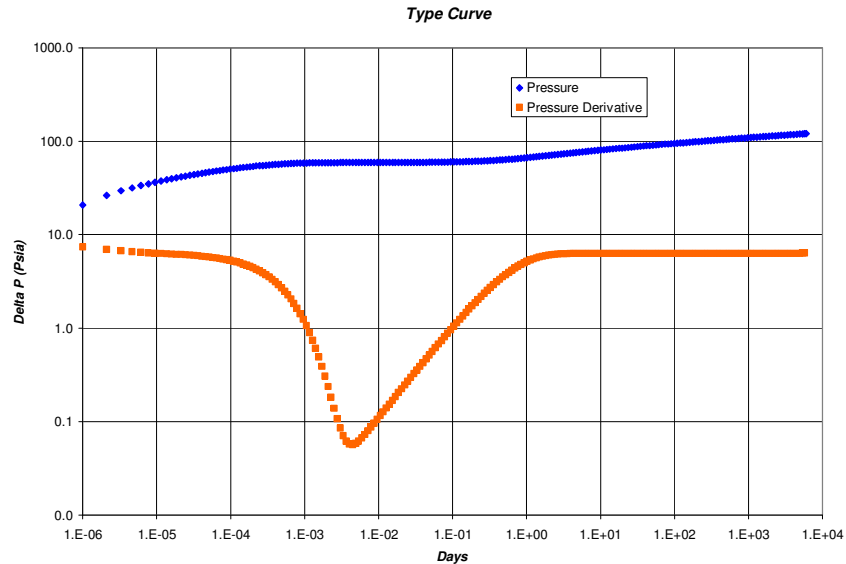

Figure. C.1 Typical Type Curve for a Naturally Fractured Reservoir.

To analyze the effect of lambda and omega variations, different cases were simulated. First, setting lambda constant (λ=0.0001). Omega was changed from 0.001 to 0.01. The results are shown in Fig. C.2.

Fig. C.3 shows the results when lambda was changed from 0.00004 to 0.0001 using a constant value for omega (0.001).
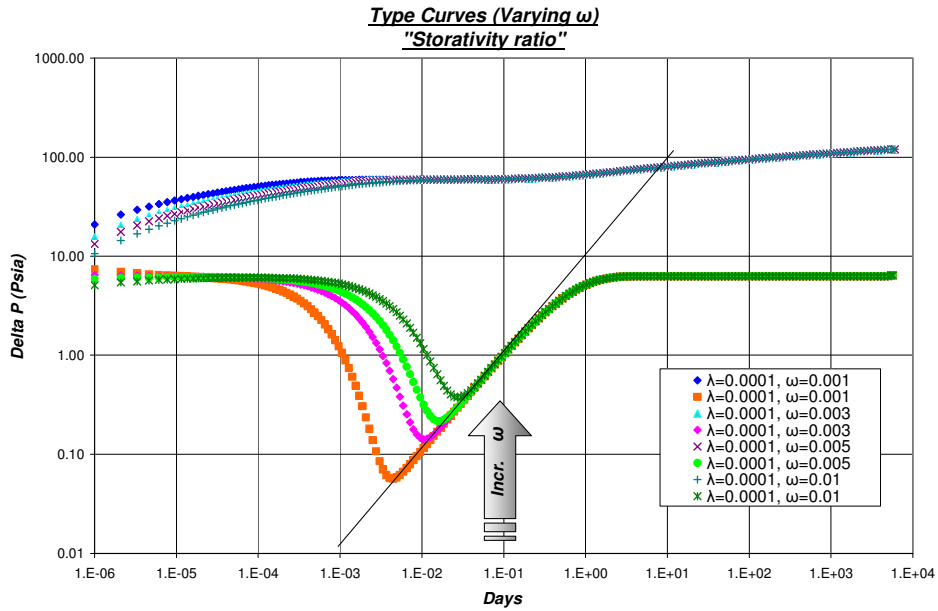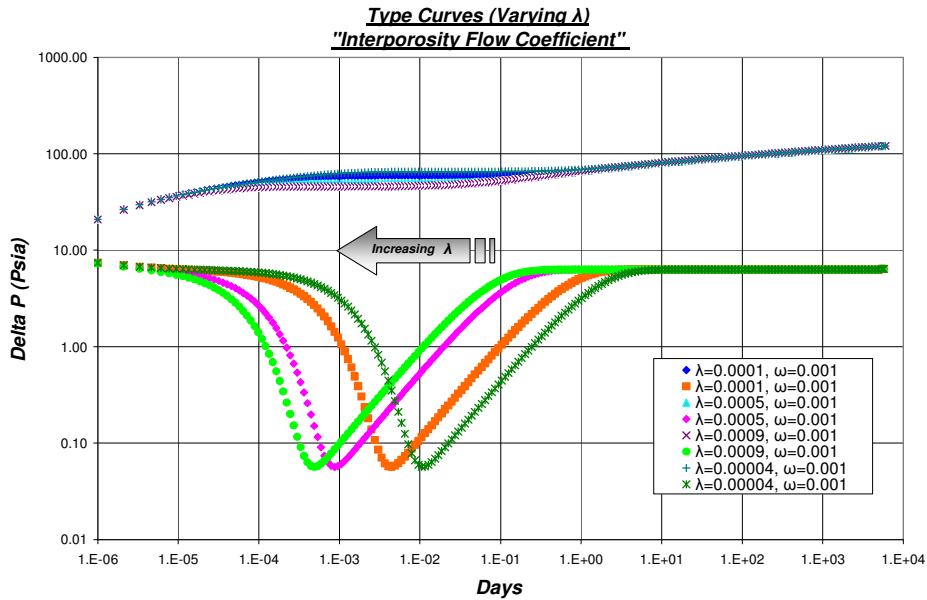
Figure. C.2 Sensitivity to Omega, *ω*.

Figure. C.3 Sensitivity to Lambda, *λ*.

VITA

Name: Carlos A. Mora

Permanent Address: Calle 120 A # 62-26 Apt. 303

Bogota, Colombia

Education: B.S., Petroleum Engineering

Universidad de America, Bogota, Colombia

M.S., Petroleum Engineering

Texas A&M University, August 2007